

AD-A035 271

OHIO STATE UNIV RESEARCH FOUNDATION COLUMBUS

F/G 11/6

FUNDAMENTAL STUDIES OF DISSOLUTION AND PASSIVITY OF ALLOYS AND --ETC(U)

NOV 76 J B LUMSDEN, R W STAEMLE

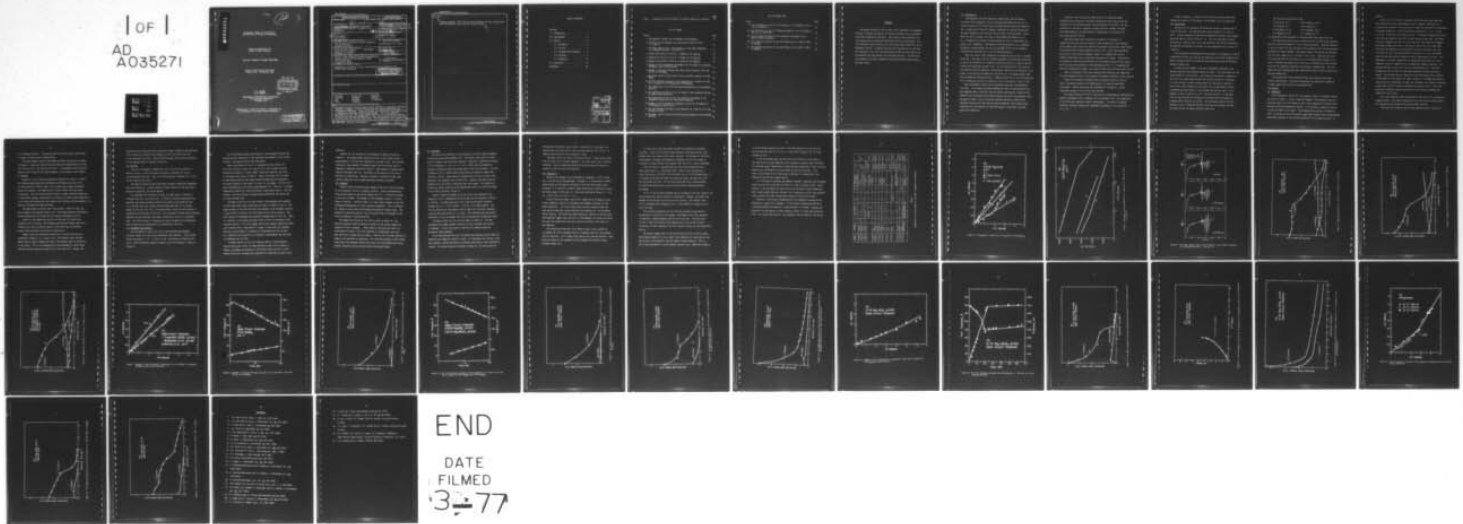
N00014-75-C-0665

UNCLASSIFIED

OSURF-4131A1-1

NL

1 OF 1
AD
A035271



ADA035271

12

J

Fundamental Studies of Dissolution
and Passivity of Alloys and Compounds

Research Program for the
Office of Naval Research

Contract # N00014-75-C-0665 (NR036-085)

Report of Work During the Period
1 March 1975 - 29 February 1976

DDC
RECEIVED
FEB 4 1977
RECEIVED

J.B. Lumsden
R.W. Staehle

Department of Metallurgical Engineering
The Ohio State University
Columbus, Ohio

Reproduction in whole or in part is permitted for
any purpose of the United States Government

DISTRIBUTION STATEMENT A
Approved for public release
Distribution Unlimited

UNCLASSIFIED

SECURITY CLASSIFICATION OF THIS PAGE (When Data Entered)

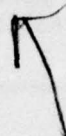
REPORT DOCUMENTATION PAGE		READ INSTRUCTIONS BEFORE COMPLETING FORM
1. REPORT NUMBER	2. GOVT ACCESSION NO.	3. RECIPIENT'S CATALOG NUMBER
4. TITLE (and Subtitle) ALLOY CORROSION - FUNDAMENTAL STUDIES OF DISSOLUTION AND PASSIVITY OF ALLOYS AND COMPOUNDS.		5. TYPE OF REPORT & PERIOD COVERED Interim Report - 1 Mar 75 - 29 Feb 76
7. AUTHOR(s) 10 J.B. Lumsden R.W. Staehle		6. PERFORMING ORG. REPORT NUMBER RF-4131-A1-1
9. PERFORMING ORGANIZATION NAME AND ADDRESS The Ohio State University Research Foundation 1314 Kinnear Road Columbus, Ohio 43212		8. CONTRACT OR GRANT NUMBER(s) 15 N00014-75-C-0665
11. CONTROLLING OFFICE NAME AND ADDRESS Office of Naval Research Department of the Navy Arlington, VA 22217 Code N00014		10. PROGRAM ELEMENT, PROJECT, TASK AREA & WORK UNIT NUMBERS NR 036-085/1-3-75 (471)
14. MONITORING AGENCY NAME & ADDRESS (if different from Controlling Office) Office of Naval Research Resident Representative The Ohio State University Research Center 1314 Kinnear Road Columbus, OH 43212		12. REPORT DATE 11 November 1976
		13. NUMBER OF PAGES 127 pages
		15. SECURITY CLASS. (of this report) Unclassified
16. DISTRIBUTION STATEMENT (of this Report) Reproduction in whole or in part is permitted for any purpose of the United States Government		15a. DECLASSIFICATION/DOWNGRADING SCHEDULE
17. DISTRIBUTION STATEMENT (of the abstract entered in Block 20, if different from Report) DISTRIBUTION STATEMENT A Approved for public release; Distribution Unlimited		
18. SUPPLEMENTARY NOTES		
19. KEY WORDS (Continue on reverse side if necessary and identify by block number) Corrosion Inhibitors Molybdate Passivity Phosphate Nitrite Iron Chromate Ellipsometry Films Tungstate		
20. ABSTRACT (Continue on reverse side if necessary and identify by block number) The growth kinetics of iron at open circuit potentials in phosphate, chromate, tungstate, molybdate, and nitrite solutions were investigated using the ellipsometric technique. These results were correlated with film compositions as determined using Auger electron spectroscopy. All films thickened logarithmically with time except those formed in a pH 9.1 phosphate solution. In general the less the incorporation of ions from oxyanions in the film, the more protective the film was found to be. The exception was that formed in the		

UNCLASSIFIED

SECURITY CLASSIFICATION OF THIS PAGE(When Data Entered)

20. cont.

chromate solution. This film was very protective and had a composition which approximated that found on stainless steels.



APPROVED FOR RELEASE
BY THE NATIONAL ARCHIVES
REF ID: A66502

UNCLASSIFIED

SECURITY CLASSIFICATION OF THIS PAGE(When Data Entered)

TABLE OF CONTENTS

Abstract

1.0 Introduction1

2.0 Experimental3

3.0 Results.4

 3.1 Chromates4

 3.2 Nitrite7

 3.3 Molybdate and Tungstate7

 3.4 Arsenate.9

 3.5 Phosphate10

4.0 Discussion11

References.36

SEARCHED	INDEXED
FILED	REF. SECTION
SERIALIZED	
EXTENDED	
<i>Letter on file</i>	
BY	
DISTRIBUTION/AVAILABILITY CODES	
Dist.	AVAIL. and/or SPECIAL
A	

	<u>Page</u>
Table I. Properties of Films Formed on Iron While Exposed to Inhibitors	14

LIST OF FIGURES

Figure	Page
1. Ellipsometric results for Fe exposed to 0.01N Na_2CrO_4 .	15
2. The open circuit potential as a function of time for films 1, 2, and 4.	16
3. The Auger spectra from a film formed at a high anodic potential in a chromate solution. (Film no. 3).	17
4. Composition profile of film no. 1 formed in 0.01 Na_2CrO_4 .	18
5. Composition profile of film no. 2 formed in 0.01 Na_2CrO_4 .	19
6. Composition profile of film no. 4 formed in 0.01 Na_2CrO_4 .	20
7. Changes in the ellipsometric parameters for Fe exposed to tungstate, molybdate, and nitrite solution.	21
8. Changes in the film thickness and open circuit potential with time for Fe in 0.1N NaNO_2 .	22
9. The Auger results of the passive film on Fe after exposure to 0.01N NaNO_2 .	23
10. The film thickness and open circuit potential as a function of time for Fe exposed to 0.01N Na_2WO_4 and 0.01N Na_2MoO_4 .	24
11. The composition of the film resulting from exposure to the molybdate solution.	25
12. The composition profile of the film formed in the tungstate solution at open circuit potentials.	26
13. The composition profile of the film formed on Fe exposed to the tungstate solution and at a high anodic potential.	27
14. Changes in the ellipsometric parameters A and P for Fe exposed to 0.1N Na_2AsO_4 at open circuit.	28
15. The film thickness and open circuit potential vs. time for Fe in the arsenate solution.	29
16. The Auger results of the film resulting from exposure to the arsenate solution.	30

LIST OF FIGURES CONT.

Figure	Page
17. The ellipsometric results for Fe exposed to 0.1N Na_2HPO_4 at open circuit potentials.	31
18. The composition of the film formed by immersion in 0.1N Na_2HPO_4 at open circuit potentials.	32
19. The ellipsometric results for Fe exposed to phosphates and at applied anodic potentials.	33
20. The composition profile of the film formed on Fe at -300 mV (SCE) in Na_2HPO_4 .	34
21. The composition profile of the film formed on Fe at 300 mV (SCE) in Na_2HPO_4 .	35

ABSTRACT

The growth kinetics of iron at open circuit potentials in phosphate, chromate, tungstate, molybdate, and nitrite solutions were investigated using the ellipsometric technique. These results were correlated with film compositions as determined using Auger electron spectroscopy. All films thickened logarithmically with time except those formed in a pH 9.1 phosphate solution. In general the less the incorporation of ions from the oxyanions in the film, the more protective the film was found to be. The exception was that formed in the chromate solution. This film was very protective and had a composition which approximated that found on stainless steels.

1.0 Introduction

Investigations into the properties, compositions, and thicknesses of surface films produced on iron in solutions manifesting the ability to inhibit corrosion are of great value in explaining the inhibition mechanism. This is particularly true for inorganic inhibitors of the passivating type. The most frequently used inhibitors can be divided into two groups: those which are able to protect iron both in the presence and absence of air, e.g., chromates and nitrites, and those which act only in the presence of oxygen, e.g., phosphates. Some weakly oxidizing oxyanions, e.g., arsenates, tungstates, and molybdates, can also be included in the list of inorganic inhibitors but they have only a very limited application.

There are several ideas attempting to rationalize the action of inorganic inhibitors. The oldest and still widely accepted one assumes that inhibition is due to the formation of a protective layer which acts as a physical barrier slowing the dissolution process (1-4). For its formation Fe^{+2} ions which go into solution from the defective sites undergo oxidation by the inhibitor or by oxygen in the solution and deposit on the anode as an insoluble product layer able to produce an adherent barrier. Another possibility is that the protective film is formed by the direct oxidation of iron in the metallic lattice (5,6).

Many experimental results can be explained using only electrochemical principals. This concept has been developed by Stern (7) and Kolotyrkin (8) who suggested that an inhibitor does not need to participate in passive film formation but accelerates the cathodic reaction and shifts the potential into the passive range. Thus an oxidizing inhibitor provides a stable mixed potential more positive than the passivating potential, while nonoxidizing inhibitors need the presence of dissolved oxygen or some other oxidizing agent to be effective.

Inhibitors which are salts of weak acids act as buffering agents preventing the occurrence of localized acidification which results from the hydrolysis of the dissolving metal from perforations in the film. The low solubility of the ferric compounds of these inhibitors further increases the effectiveness by the precipitation or deposition of insoluble salts, thus repairing the film (9).

Additional ideas which rationalize the action of inhibitors in suppressing corrosion rates are based on their adsorption at the interface. Uhlig suggests that these ions chemisorb on the metal surface thus immobilizing the electrons which reduces chemical activity (10). While other mechanisms are based on electrostatic arguments, where it is assumed that the most effective inhibitors have a nonuniform distribution of charge. These anions are assumed to adsorb electrostatically on the filmed surface and thus attract and tie up any free electrons in the semiconducting film. It is hypothesized that this induced field hinders the escape of metal ions from the surface (11,12).

There is relatively little work concerning the thickness and composition of films produced on iron in the presence of inorganic inhibitors in the solution.

Kruger (13) studied ellipsometrically the growth of passive films on iron in an aerated solution of 0.0025M K_2CrO_4 . He observed logarithmic film growth. Similar tests were also performed in 0.1M $NaNO_2$, in which logarithmic growth of the film was also observed.

The growth kinetics of films on iron was also investigated by Smialowska and Staehle in phosphates (14), chromates (15) and arsenates (16). The composition of the films was studied by several investigators. In case of a chromate inhibitor, indirect evidence has indicated the presence of Cr in the film (1, 3, 17).

There are, however, no studies in which correlations have been made between the kinetics of film growth, its thickness, and its composition.

2.0 Experimental

Cylindrical iron specimens (99.99% purity) having an exposed area of 0.32 cm^2 were used. The specimens were vacuum annealed for 3 hours at 750°C . Surface preparation consisted of mechanical polishing using diamond abrasives down to a final finish of $1 \mu\text{m}$. This was followed by electro-polishing in a glacial acetic acid, 70% perchloric acid (20:1) electrolyte. The specimen was exposed for 25 hours at room temperature and a current of μ ohms/cm.

The ellipsometric measurements were performed at a wavelength of 5461 \AA . A description of the cell used and the apparatus can be found elsewhere (18). Optical constants and film thicknesses were determined using the McCrackin computer program (19).

In each case the changes in the two ellipsometric parameters, the analyzer angle and the polarizer angle, are given. The curves shown are the least squares fit to the points. Also given are the optical constants of the film, $n-ik$, which would satisfy this locus of points as it thickens. It is not possible to obtain unique values for the optical constants; thus in most cases several are given which fit the experimental results. In determining these values, it was assumed that the real part, n , lay between 1.5 and 2.6 and $0 \leq k \leq 0.4$. The value $2.6-0.4 i$ is the upper limit of that obtained for the passive film resulting from exposure to a borate buffer solution (18, 20-22). The calculated value of the film thickness is not a sensitive function of the optical constants varying less than 15% for the ranges given for each curve.

The following solutions were used:

0.1N Na_2CrO_4 , pH 12	0.05 N Na_2WO_4 , pH 8.5
0.1N Na_2CrO_4 , pH 7	0.01 N NaNO_2 , pH 7
0.1N Na_2HAsO_4 , pH 8.6	0.01 N Na_2HPO_4 , pH 9.1
0.1N Na_2MoO_4 , pH 9.6	0.1 N Na_3PO_4 , pH 12

All measurements were performed in solutions which were open to the air.

The specimen was polarized to a potential which was 300 mV more negative than the corrosion potential of iron in the given medium. Cathodic reduction of the air-formed film was continued at this potential until the ellipsometric parameters no longer changed. The complex index of refraction thus obtained was $3.0-4.20i$, where $n=3.0 \pm 0.05$ and $k = 4.2 \pm 0.15$. Comparing this with the value obtained for film free iron in an ultrahigh vacuum system, ($3.35 - 3.85 i$) indicates the presence of a very thin air-formed film on the surface which was not completely reduced by the cathodic treatment (23). Thus for comparison some investigations were undertaken without initially treating the specimen cathodically.

The compositions of the protective films were obtained using Auger electron spectroscopy. The profiling technique was used which allowed the in-depth composition profiles to be obtained (24).

3.0 Results

3.1 Chromates

The ellipsometric results for iron exposed to the pH 7 chromate solution are given in Figure 1. Curve 1 shows the changes in the analyzer angle and polarizer angle, for films formed at open circuit potential on surfaces which had been initially cathodically reduced. A film having a refractive index of 1.6 can be fitted to this curve. The thickness after one hour of growth is 58 \AA . The growth of this film follows logarithmic kinetics with a corresponding logarithmic decrease in the corrosion potential (17) as shown by curve 1 in

Figure 2.

Curves 2 and 4 of Figure 1 represent films which were grown under the same conditions as that represented by curve 1; however, different ΔA vs. ΔP curves were obtained. The variations in slope are indicative of differences in optical properties. Films having optical properties $n = 1.6 - 1.9$ and $k = 0.018 - 0.076$ could be fitted to curve 2. Thicknesses ranged from 45-58 Å after one hour depending upon which optical constants were used. The shape of curve 4 suggests that this is a two layer film; the slope of the segment which goes through the origin is the same as that of the iron oxide films resulting from exposure to a borate buffer solution; assuming a two layer film with the first layer having optical constants $2.6 - 0.3i$, the second layer has the same optical constants as those represented by curve 2. This hypothesis is further supported by the observation that curve 4 is also obtained if the air formed film is not removed by cathodic reduction. The maximum thickness of the first layer was approximately 10 Å. The total thickness of the two-layer film was approximately 40 Å after one hour of growth. The different optical properties can be correlated with variations in the potential-time behavior as shown in Figure 2. Although the slopes of these curves are essentially the same, the intercepts are different indicating a more rapid initial increase in potential for curves 2 and 4. Thus, the potentials under which steady state growth is occurring are substantially higher for films 2 and 4.

Film 3 was formed by anodic polarization at 700 mV SCE on a cathodically reduced surface. The optical constants of this film were the same as those for the passive film formed in the borate buffer solution.

Films were also formed at open circuit potentials and at 700 mV in a

pH 12 chromate solution. The optical results were the same as those shown in Figure 1 (curves 2 and 3 respectively).

The Auger spectra from the film formed by anodic polarization are shown in Figure 3. Spectra are shown from the surface, and approximately 15 Å and 25 Å into the film. The film was 30 Å thick. In accordance with the optical results, the film was an iron oxide; however, it did contain a small amount of chromium.

Figures 4, 5, and 6 show the composition profiles for films 1, 2, and 4. The indicated Auger peaks were normalized by dividing by the sum of the Fe 703 eV and the Cr 519 eV lines. All of these films contain substantial amounts of chromium. The composition of film #1 differs from the others in two ways: first the surface region contains a higher chromium content and a lower oxygen content, second there is a region of constant oxygen composition. In all cases the chromium and iron contents vary inversely with one another, i.e., where one increases the other decreases.

The compositions of films 2 and 4 are the same. These are much like those formed on the stainless steels (15). The oxygen decreases continuously, and the chromium and iron levels are not constant throughout the film.

Figure 5 is the composition profile for the type 2 film which was formed in a pH 12 solution. No difference was detected between those films formed in pH 7 and 12 solutions except in the latter case the chromium content (the area under the curve) was slightly less.

Figure 6 gives the composition profile for a surface which was not cathodically reduced, i.e., a type 4 film. The chromium signal vanished before that of oxygen although the level of the oxygen signal was quite low at this point. This is in accordance with the ellipsometric results which indicate that the underlying oxygen film is less than 10 Å. However, the

possibility exists that nonuniform sputtering creates islands of the overlying film in the area of analysis and chromium is driven into the oxide film by the impinging argon ions. Both of these processes would cause an increase of the apparent depth of chromium in the film.

3.2 Nitrite

The $\Delta A - \Delta P$ ellipsometric response for iron in the nitrite solution is shown in Figure 7. This is the same curve which is obtained for iron in the borate buffer solution. Thus a film having optical constants $2.6 - 0.21 i$ can be fitted to this curve.

The potential decay and the film growth followed a logarithmic dependence with time (Figure 8). A unique feature of these results was the very rapid decrease in potential, 270 mV per decade.

In accordance with the optical results the Auger analysis (Figure 9) indicates that this is an oxide film. No region of constant composition was observed; the oxygen decreased uniformly and rapidly with sputtering time. It is unlikely that such a region would be detectable even if it existed because of the very thin film. The escape depth of the Fe 703 eV electrons is approaching the thickness of the film. Thus some Auger electrons would originate detected from the substrate, the number increasing as the film is sputtered away. The relative amount of oxygen would then also appear to be decreasing. Some nitrogen was also observed to be incorporated in the film.

3.3 Molybdate and Tungstate

The ellipsometric results for iron in the tungstate and molybdate solutions (Figure 7) at open circuit potentials were identical. Films having optical constants $n = 1.6 - 1.9$ and $k = 0.02 - 0.04$ could be fitted to this curve. The corresponding change in potential and film thickness is shown in Figure 10.

The film formed by anodic polarization in the molybdate solution had the same optical properties as that resulting from exposure to the nitrite solution. The growth kinetics were logarithmic.

Anodic polarization of iron in a tungstate solution results in a $\Delta A-\Delta P$ curve similar to that for a type 4 film in the chromate solution provided the potential is above -100mV. Below this potential the curve is the same as that shown in Figure 7. Hence a two layer film is formed at high anodic potential each layer having different optical properties. The growth kinetics of the anodic film occur in two stages. The film first grows logarithmically with time to approximately 10 \AA . Then 0.5 - 15 seconds (depending on potential) after polarization, rapid growth occurs. The film reaches a limiting thickness of approximately 250 \AA after 100 seconds and no longer thickens (25).

The Auger results for the films formed in the molybdate and tungstate solution under open circuit conditions are shown in Figures 11 and 12. The oxygen content of the film resulting from exposure to the molybdate solution is very similar to that for the film formed in the nitrite solution. Very small amounts of molybdenum were detected throughout most of the film. There is a shoulder in the normalized oxygen curve for the film produced in the tungstate solution. The first segment follows the tungsten composition which could indicate that a large amount of oxygen is associated with tungsten. Relatively large amounts of tungsten are concentrated near the surface. As a comparison the sensitivity to tungsten is approximately one-half that of molybdenum and iron (26).

The Auger results for the film formed at 500 mV in the molybdate solution were quite similar to those obtained at open circuit potential. However, molybdenum was detected in the surface layers only and in small amounts which never exceeded those obtained for films grown at open circuit

potential.

Results for iron polarized in 0.05N Na_2WO_4 at 900 mV are shown in Figure 13. The oxygen content relative to iron, in the surface layers is approximately 2 1/2 times that obtained for the other films. This and the presence of large amounts of tungsten suggest that the surface layer is composed of compounds containing Fe and W. Large amounts of tungsten were detected throughout the film. The nature of the interior of the film is difficult to rationalize. Tungsten is present in relatively large, near constant quantities, while oxygen decreases uniformly with depth.

3.4 Arsenate

Figure 14 gives the relationship between ΔA and ΔP for the film formed on iron exposed to the pH 8.6 Na_2HAsO_4 solution. Curves corresponding to films having indices of refraction ranging from 1.6 - 1.74 could be fitted to this set of points. The changes in film thickness (using $n = 1.6$) are shown in Figure 15. Initially there is a steep linear increase in the film thickness corresponding to a sharp increase in potential. This is followed by a region in which both film thickness and potential change slowly. The potential at which the onset of slow film growth occurs corresponds to the critical potential of passivation (16).

The composition profile of this film is given in Figure 16. The high O/Fe content and the existence of arsenic on the surface suggest the presence of ferric arsenate. Auger analysis indicates that there is a large amount of arsenic since this technique is approximately ten times more sensitive to oxygen than to arsenic. There is also an abrupt decrease in oxygen as the substrate is approached. The continued presence of high arsenic levels after this decrease implies that arsenic was electrodeposited during cathodic reduction onto the surface before oxide growth began.

3.5 Phosphate

The open circuit behavior of iron exposed to a pH 12.3 sodium phosphate solution has been given elsewhere (14). The results were similar to those given in Figure 8 for the nitrite solution. There was a logarithmic increase in film thickness ($n = 2.6 \pm 0.1$ $k = 0.21 \pm 0.05$) and a corresponding increase in potential which was proportional to the film thickness. The film thickened to 12 \AA in 1000 minutes during which the potential ranged from -890 mV to -520 mV. Auger analysis indicated that this was an oxide film; phosphorus was detected on the surface only. However, the signal level of phosphorus was two orders of magnitude less than oxygen. The composition profile was almost identical to the composition profile for the film formed in the nitrite solution (Figure 7).

Figure 17 shows the changes in ΔA and ΔP for films formed on iron exposed to a pH 9.1 phosphate solution at open circuit potentials (-900 mV to -750 mV). As shown previously, (14) films having optical constants ranging from 1.4 - 1.5 for n and 0 - 0.14 for k fit these results. The film was found to be very complex since a single set of optical constants could not be fitted to the $\Delta A - \Delta P$ curve. This indicated that the optical properties of the film changed with time as the potential become more noble.

The Auger results for this film are shown in Figure 18. The high phosphorous and oxygen content (relative to iron) indicates the presence of phosphate. Also as the layers of the film are removed oxygen and phosphorus change together.

It has been observed that the film growth rate decreased sharply when the potential was stepped to -300 mV or above. To investigate this further, films were formed at -300 mV and +300 mV on surfaces which had not been cathodically reduced. The optical results are shown in Figure 19. The curve cannot be

extrapolated through the origin which is indicative of a two layer film. Assuming that the inner layer is the iron oxide passive film: the $\Delta A - \Delta P$ segment representing this film connects as shown.

The Auger results are shown in Figures 20 and 21. These results imply that the outer film is ferrous phosphate. The inner oxide film is clearly indicated. Thus the decreased growth rate resulting from an increase in potential is due to oxide film formation.

4.0 Discussion

Based on the changes in the ellipsometric parameters, A and P, three sets of curves can be distinguished. Although it is not possible to obtain unique values for the optical constants of the films which these curves represent, it is possible to obtain ranges of physically significant values. The three groups of films are: (1) those with refractive indices 1.7 - 2.6, (2) n from 1.6 to 1.9, (3) $n \sim 1.4$.

Films of the first group form in pH 7 NaNO_2 and pH 12 Na_3PO_4 at open circuit potential, and also in chromates and molybdate solutions at high anodic potentials. The films formed under the above conditions have the same optical properties as those resulting from exposure to a pH 8.4 borate buffer solution. The latter have been extensively studied (18, 20-24); most investigations suggest that the film is a heterogenous iron oxide with ferric ions near the surface and a mixture of ferric and ferrous ions closer to the substrate.

The second group comprises films formed at open circuit potentials in chromate (pH 8-12), molybdate (pH 9.6), tungstate (pH 8.6), and arsenate (pH 8.5) solutions. All of these films contain ions from the solution. That which was formed in the chromate solution resembles the passive film on stainless steels (27).

All the films in the last group resulted from exposure to phosphate solutions. These films thicken rapidly and grow to thicknesses many times greater than those formed in the other solutions. The presence of relatively large amounts of oxygen and phosphorous throughout the film and oxygen in solution to oxidize ferrous ions suggests that this film is ferric phosphate.

The first group is characterized by a high field ($32-35\text{mV}/\text{Å}$) and a small growth rate ($3 - 10 \text{ Å}/\text{decade time}$). While in the second group a lower field exists ($2-20 \text{ mV}/\text{Å}$), and the growth rate is $15-130 \text{ Å}/\text{decade time}$. It is interesting to note the lower the refractive index, the lower the field and the thicker the film. For the third group the field is approximately $0.03 \text{ mV}/\text{Å}$, and there exists a growth rate of several thousand angstroms per decade.

In all of the solutions examined (except arsenate in the first stage of the growth process) the growth kinetics are logarithmic. However, the growth rate depends on the species and on the pH of the solution. The thickest films form in arsenates and in Na_2HPO_4 of pH 9.1, the thinnest in Na_3PO_4 of pH 12, and in nitrates.

The protective properties of the films may the best be qualified by the potential rise per Å of film growth. The highest rise of the potential is observed in sodium phosphate (pH 12) and in nitrites. The data given in Table I show that surface films composed only of iron oxide, without inclusions of other components from the solution, exhibit the best protective ability.

The results suggest that in the case of passive films of the 1st group the oxidation process of iron at open circuit potential is rapid owing to the rapid shift of the potential into the range of oxide formation. This is due to the occurrence of a rapid cathodic reaction (e.g., reduction of NO_2^-) or

to the buffering properties as well as the high alkalinity of the solution and low corrosion rate of iron (e.g., in the case of Na_3PO_4 of pH 12 in the presence of air).

As for the second group, we think that the corrosion of iron leads to the formation of ferrous hydroxide, which undergoes oxidation under the effect of dissolved oxygen, forming ferric hydroxide and oxyhydroxide. Other oxidizing species such as chromates can also oxidize the ferrous hydroxide. This leads to the formation of a mixed oxide, hydroxide, or oxyhydroxide films containing iron and the reduced species.

It is not easy to speculate now whether arsenates, tungstates and molybdates enter into the film in the form of salts or in that of oxides as well. Nevertheless, it can be argued that such films block the metal surface effectively and a longer growth time and a thicker film is necessary to attain the potential range at which the oxides having better protective ability are formed.

Similarly, in the case of phosphates the iron phosphate produced during corrosion is a good ionic conductor. A film several thousand angstrom thick is attained before the potential of oxide formation is reached. Stepping the potential into the region of oxide formation results in a much more protective film. This occurs even after an iron phosphate film has formed on the surface.

Solution composition	Experimental conditions	pH	Optical parameters		Field m/\bar{A}	Growth rate μ/decade	Assumed composition of film from ellipsometric and electrochemical measurements	Auger analysis	this work and (13)
			n	k					
0.01 N H_2CrO_4 (1 type)	open circuit potential	8 - 12	1.6		3	33	mixture of iron hydroxide /oxyhydroxides/ and chromium hydroxides/oxyhydroxides	O, Fe and substantial amount of Cr	this work and (13)
0.01 N H_2CrO_4 (2 type)	open circuit potential	8 - 12	1.6 - 1.9	0.018 - 0.076	17.5 - 28	20 - 30	oxide film	near the substrate lack of Cr	this work and (13)
0.01 N H_2CrO_4 (4 type)	open circuit potential	8 - 12	first film: 2.6 second film: 1.7	0.31	7.5	20	mixture of iron and chromium hydroxides (oxyhydroxides)	O, Fe and Cr	this work and (13)
0.01 N H_2CrO_4 (3 type)	anodic potential	8 - 12	2.6	0.31			oxide film	O, Fe, small amount of Cr	this work and (13)
0.01 N H_2SO_4	open circuit potential	7	2.6	0.21	32	10	oxide film	C, Fe, small amount of N	this work
0.1 N H_2SO_4	open circuit potential	9.6	1.6 - 1.9	0.02 - 0.04	13.5	15	iron hydroxide (oxyhydroxide)	C, Fe, small amount of Mo	this work
0.05 N H_2NO_4	open circuit potential	8.5	1.6 - 1.9	0.02 - 0.04	13.5	15	iron hydroxide (oxyhydroxide)	O, Fe, substantial amount of N	this work
0.05 N H_2NO_4	anodic potential	8.5						O, Fe, large amount of N	this work
0.1 N $\text{H}_2\text{H}_2\text{SO}_4$	open circuit potential	8.6	1.6 - 1.74		first layer 2.1 second layer 1.9	5, 5/1 min	first layer arsenic	arsenic deposited on the metal surface	this work and (19)
0.1 N H_2PO_4	open circuit potential	12	2.6	0.21	35	5	iron hydroxide (or hydroxide)	O, Fe, As	this work and (18)
0.01 N $\text{H}_2\text{H}_2\text{PO}_4$	open circuit potential	9.1	1.4 - 1.45	0.094	0.03	several thousand	oxide film	O, Fe, P only on the surface	this work and (18)
0.01 N $\text{H}_2\text{H}_2\text{PO}_4$	anodic potential +500 and -300 mV SCE	9.1	first layer 2.6 second layer 1.5	first layer 0.21 second layer 0.02			iron phosphate	C, Fe, F	this work and (18)
							iron oxide	O, Fe	this work and (18)
							mixture of iron hydroxide and iron phosphate	O, Fe, P	this work and (18)

TABLE I
Properties of Films Formed on Iron While Exposed to Inhibitors

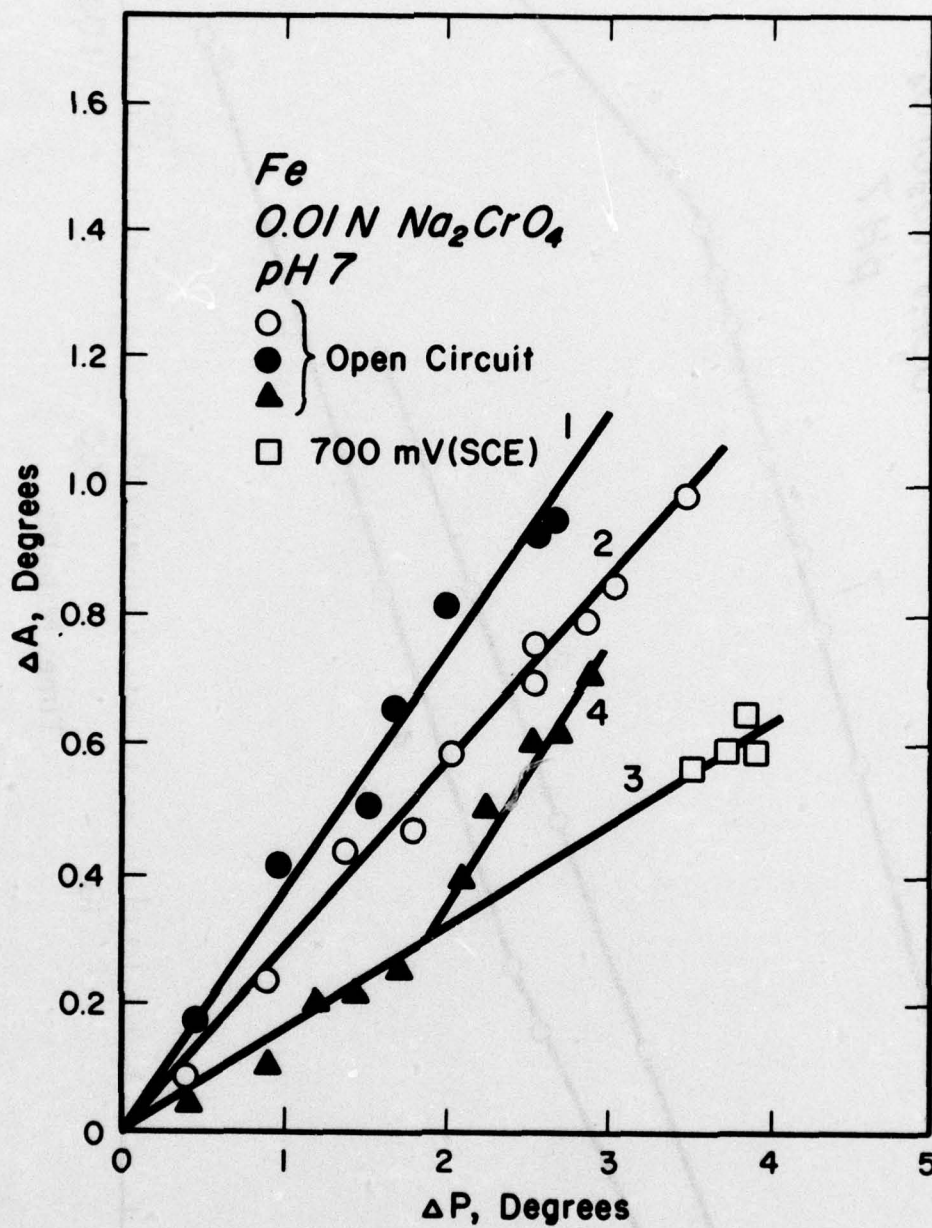


Figure 1 Ellipsometric results for Fe exposed to 0.01N Na₂CrO₄.

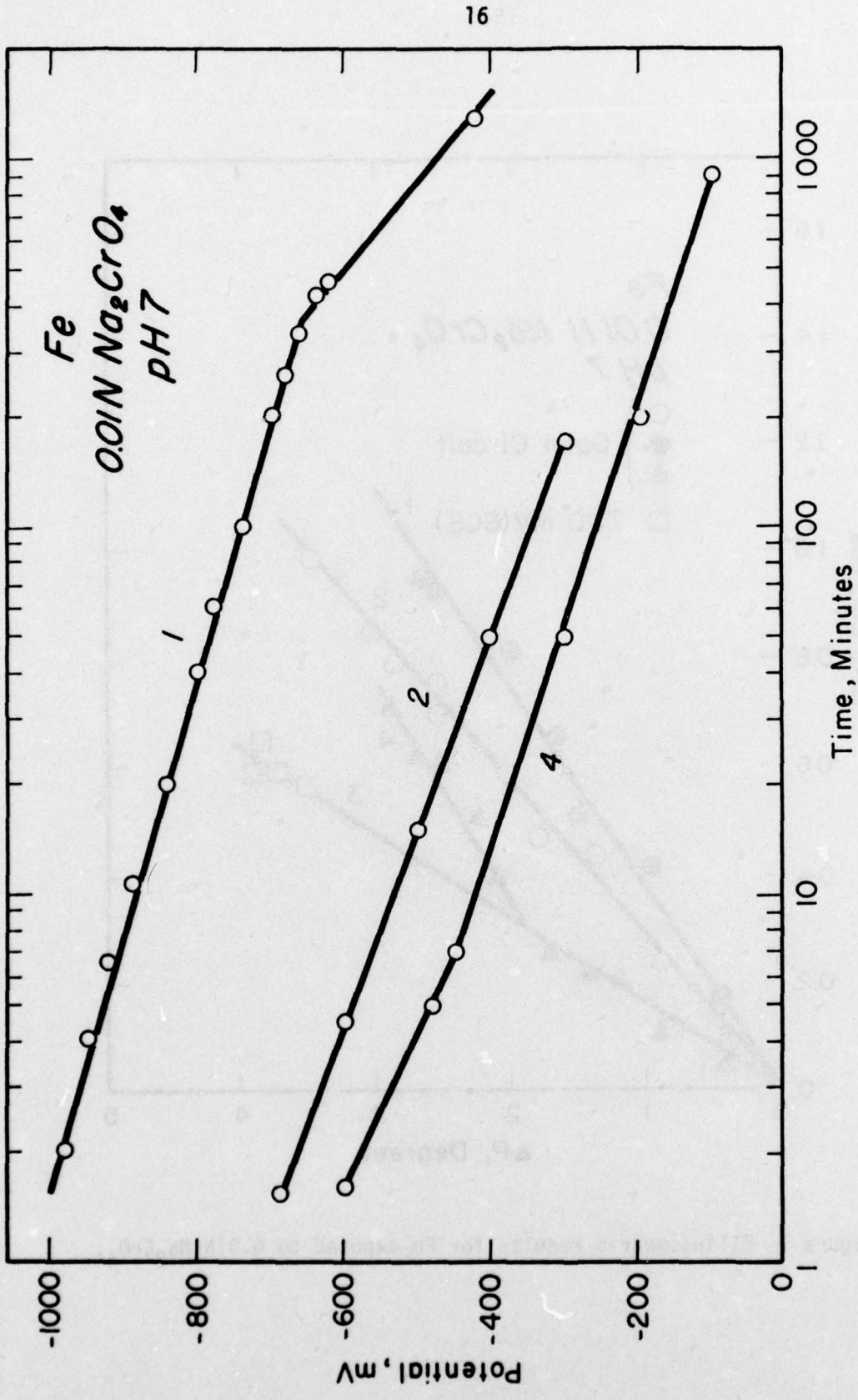


Figure 2 The open circuit potential as a function of time for films 1, 2, and 4.

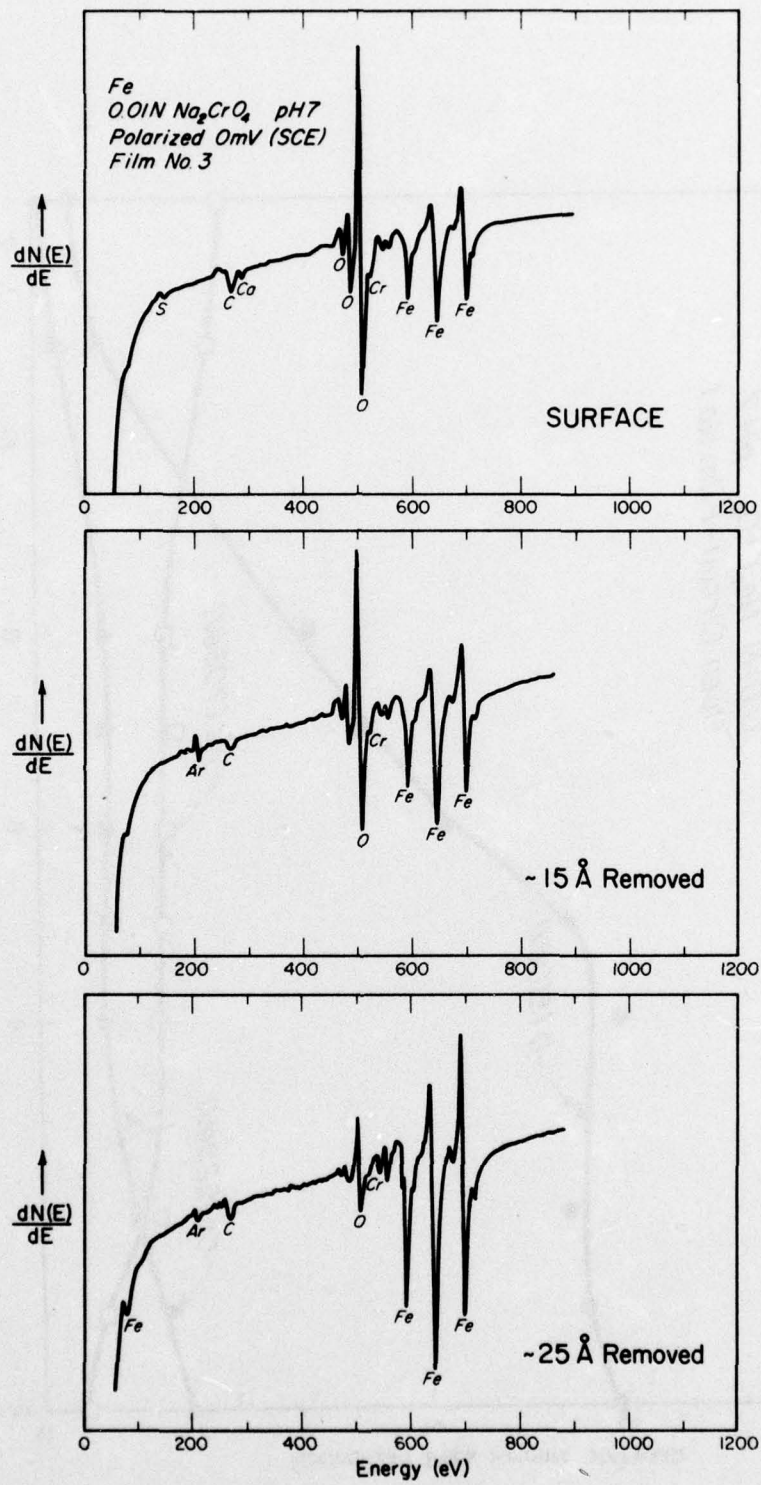


Figure 3 The Auger spectra from a film formed at a high anodic potential in a chromate solution. (Film no. 3).

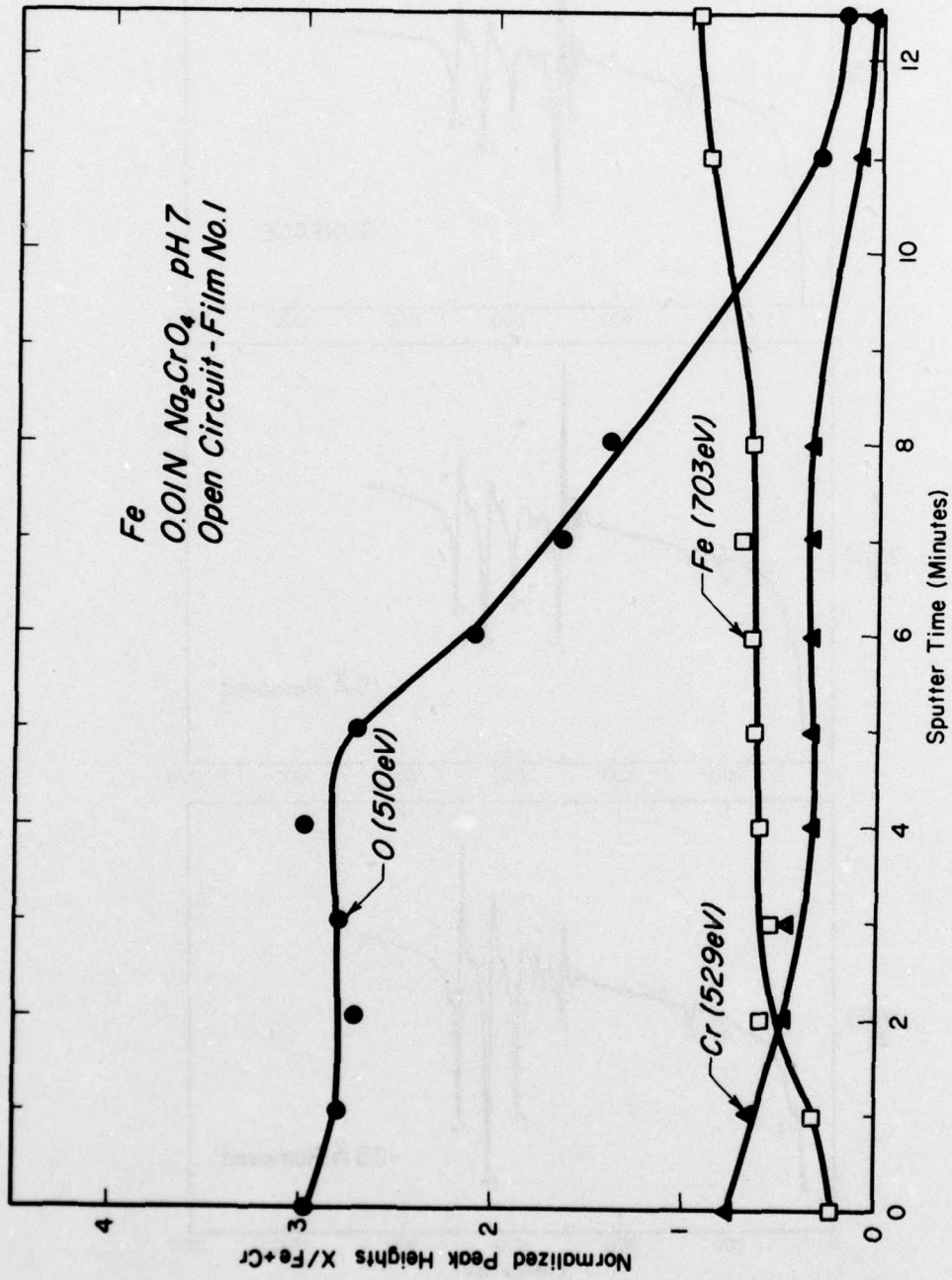


Figure 4 Composition profile of film no. 1 formed in 0.01 Na₂CrO₄.

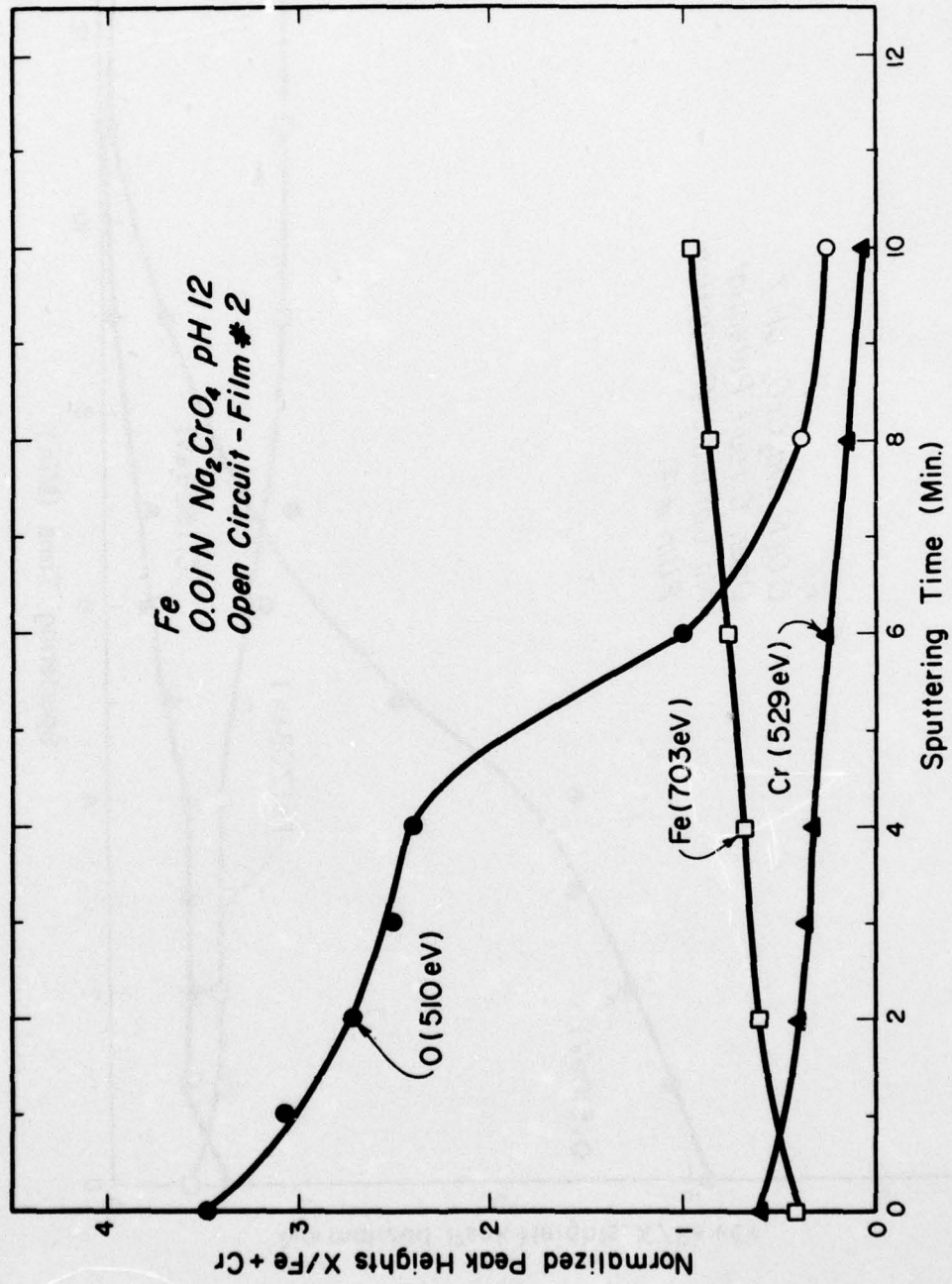


Figure 5 Composition profile of film no. 2 formed in 0.01 Na₂CrO₄.

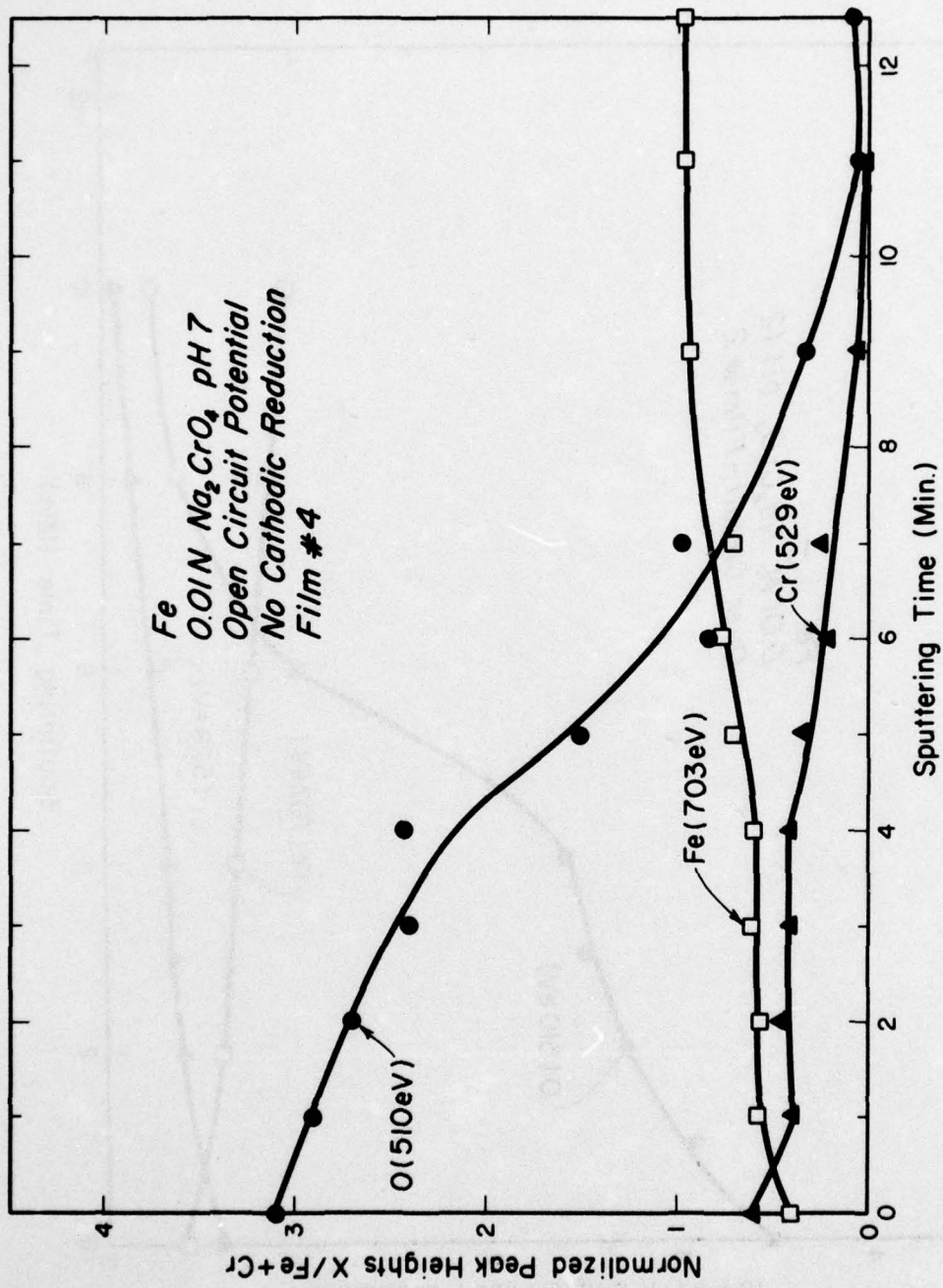


Figure 6 Composition profile of film no. 4 formed in 0.01 Na_2CrO_4 .

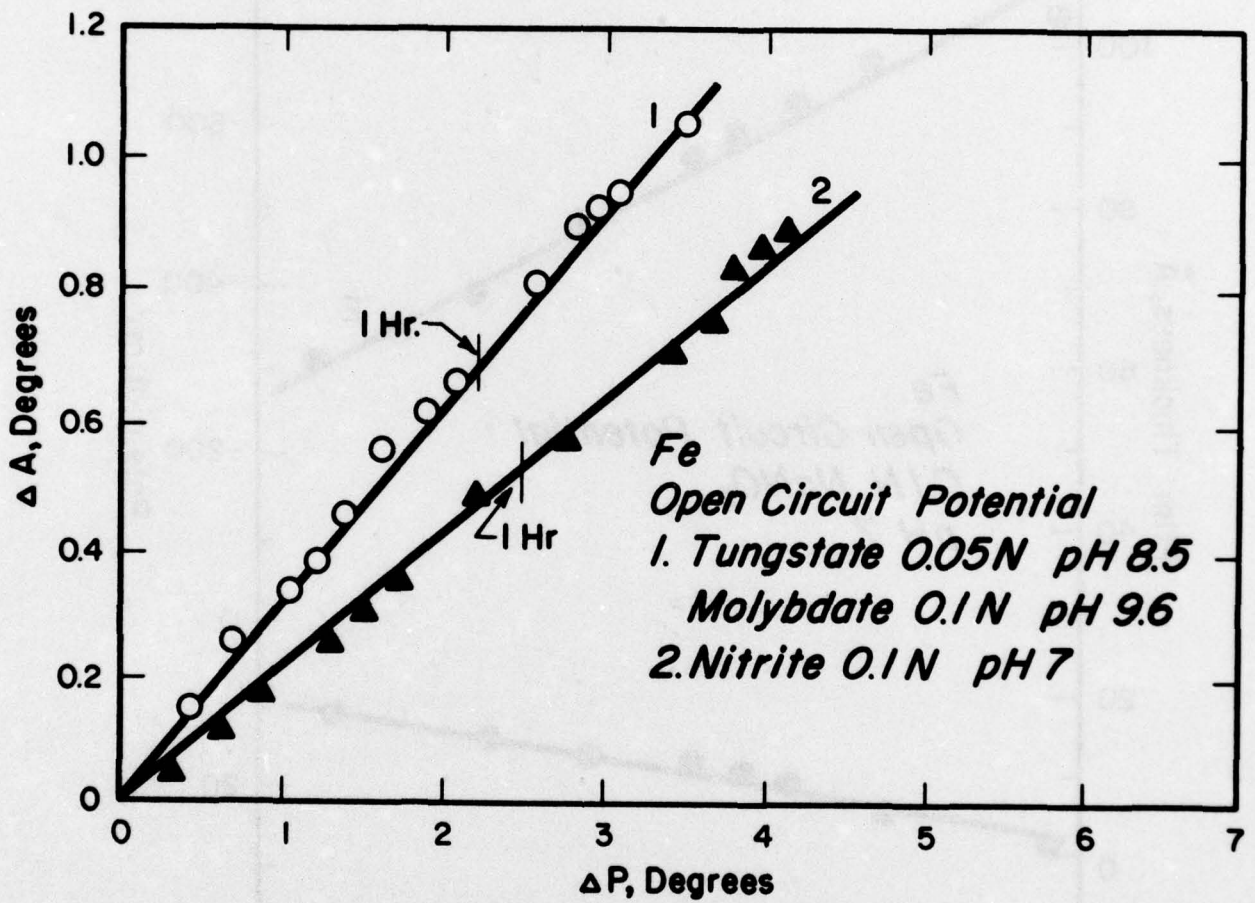


Figure 7 Changes in the ellipsometric parameters for Fe exposed to tungstate, molybdate, and nitrite solution.

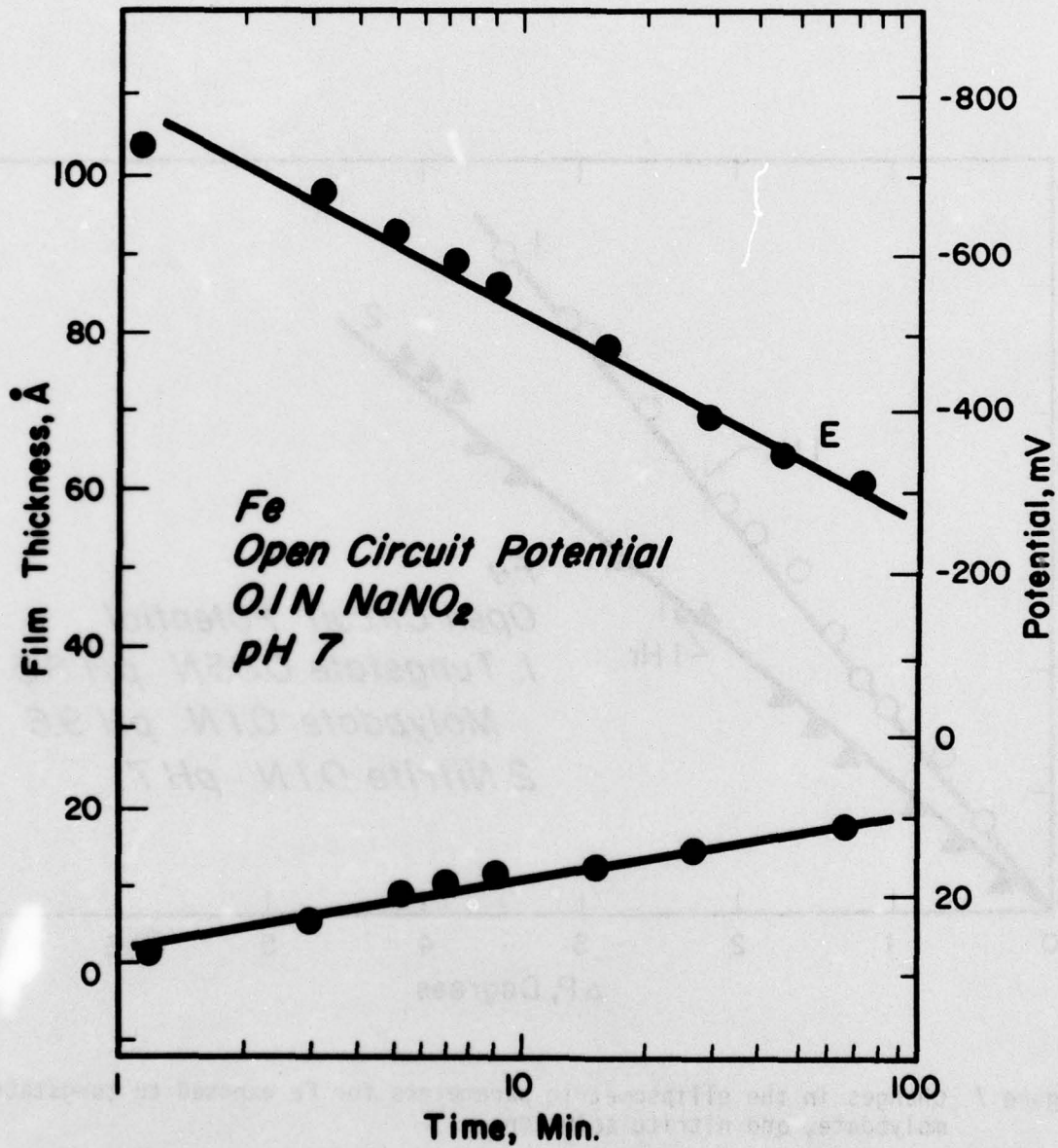


Figure 8 Changes in the film thickness and open circuit potential with time for Fe in 0.1N NaNO₂.

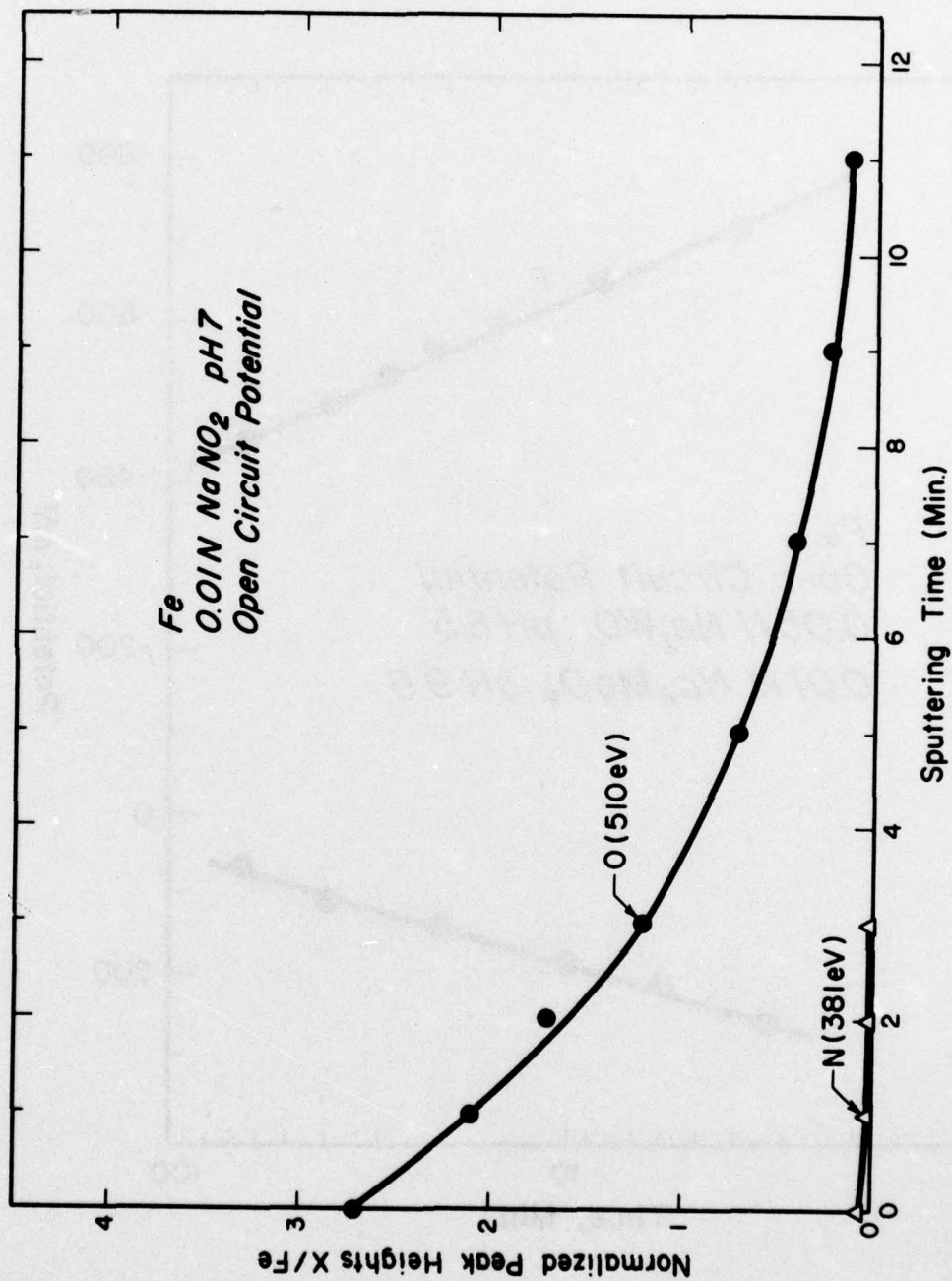


Figure 9 The Auger results of the passive film on Fe after exposure to 0.01N NaNO₂.

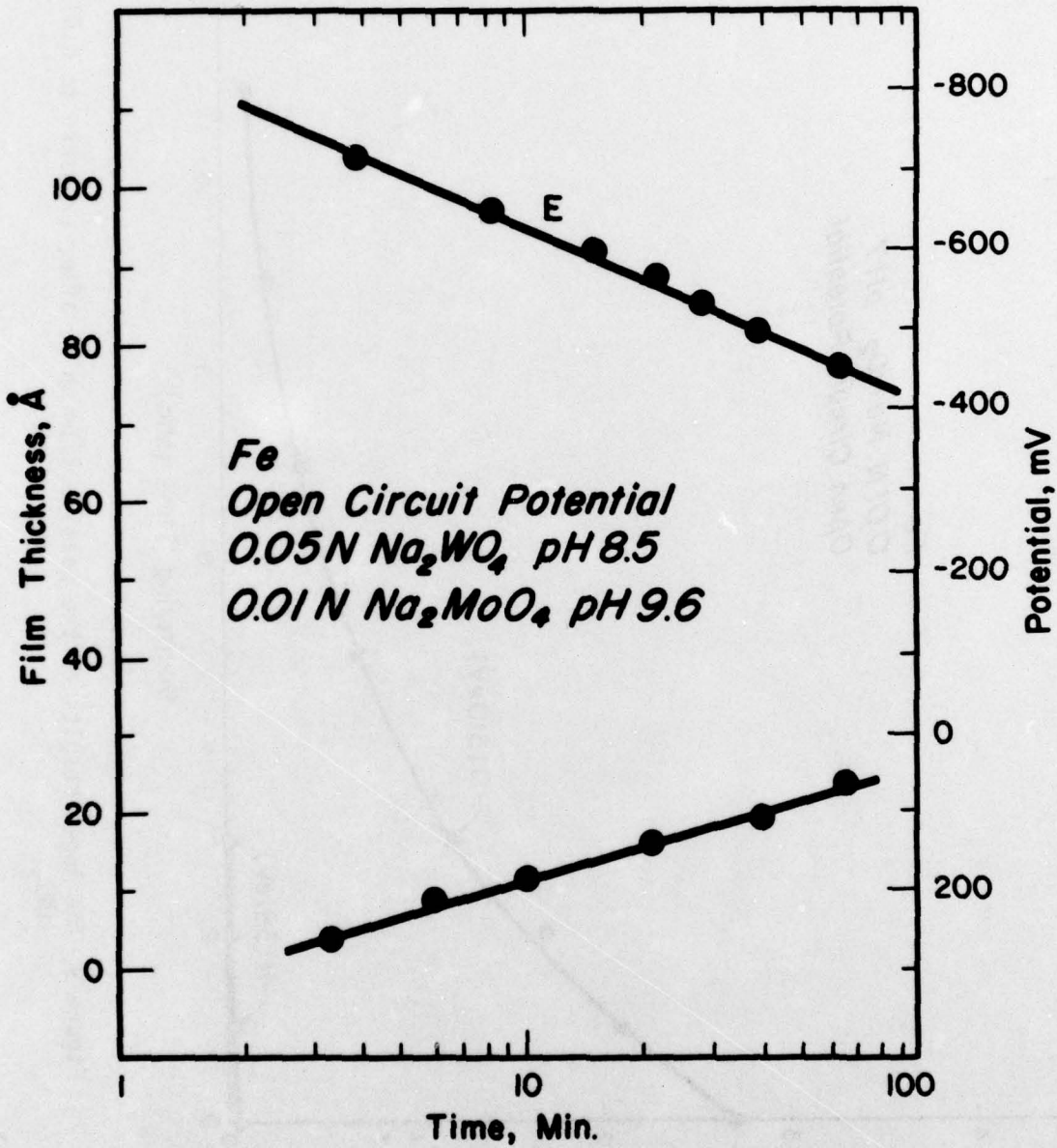


Figure 10 The film thickness and open circuit potential as a function of time for Fe exposed to 0.01N Na₂WO₄ and 0.01N Na₂MoO₄.

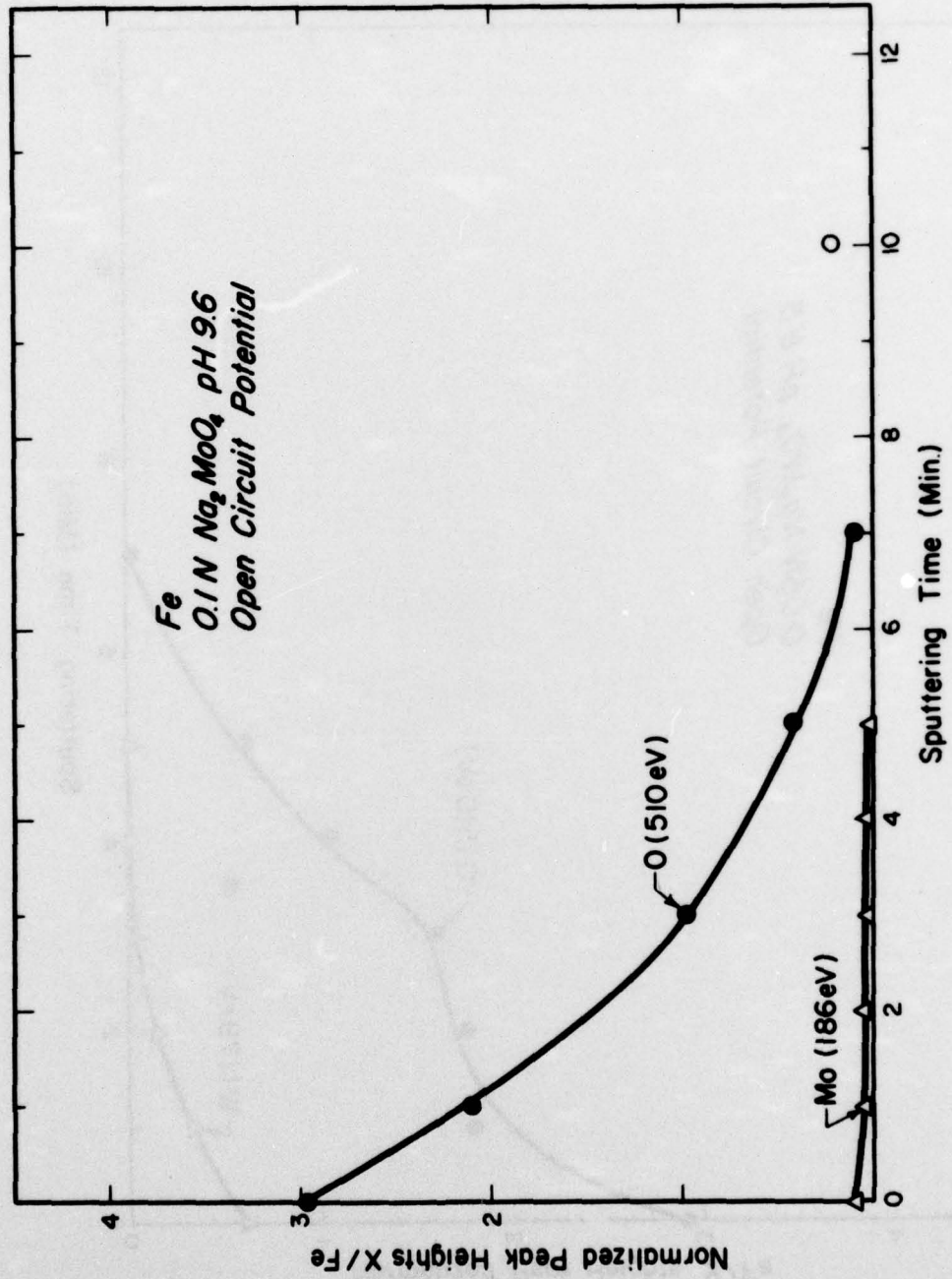


Figure 11 The composition of the film resulting from exposure to the molybdate solution.

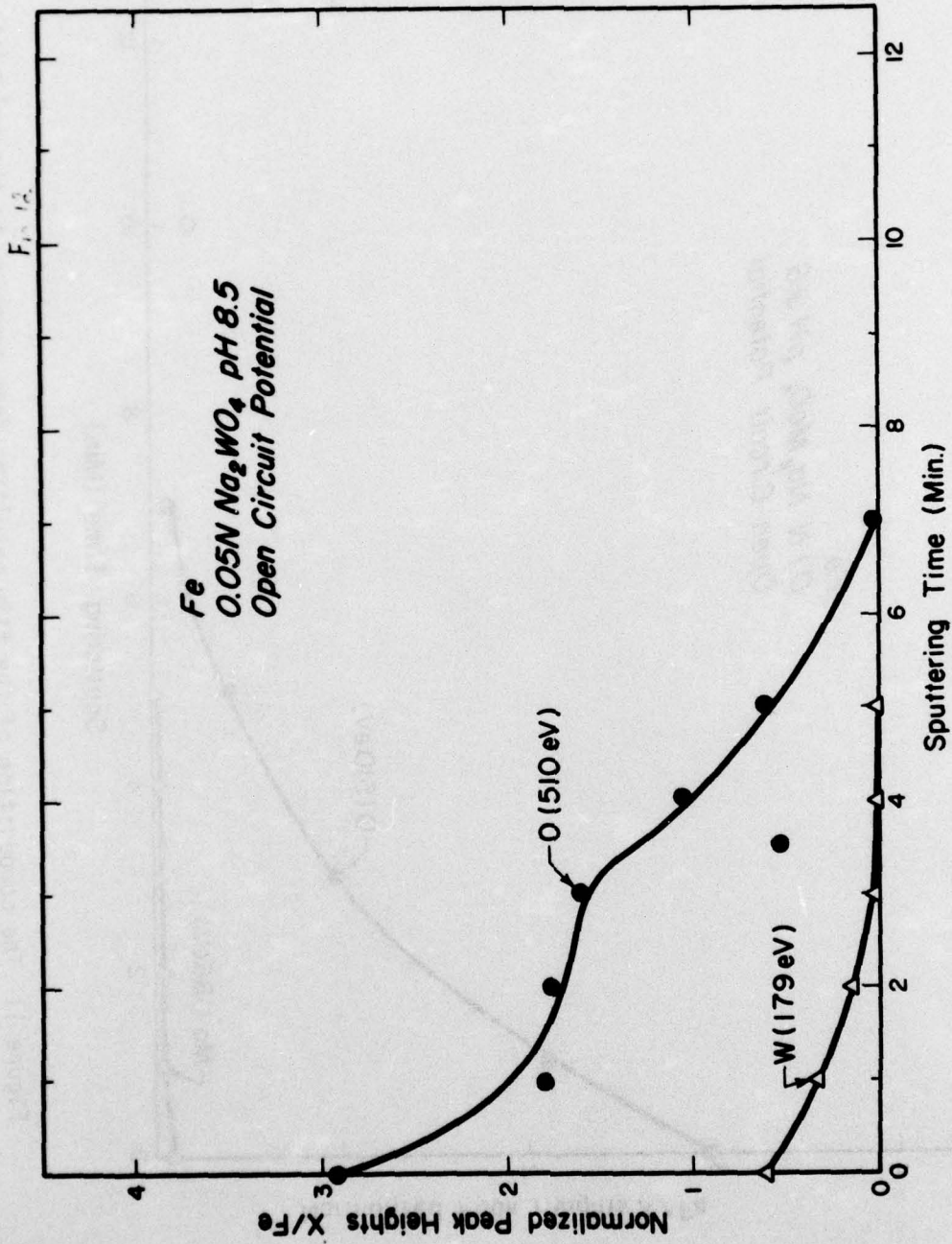


Figure 12 The composition profile of the film formed in the tungstate solution at open circuit potentials.

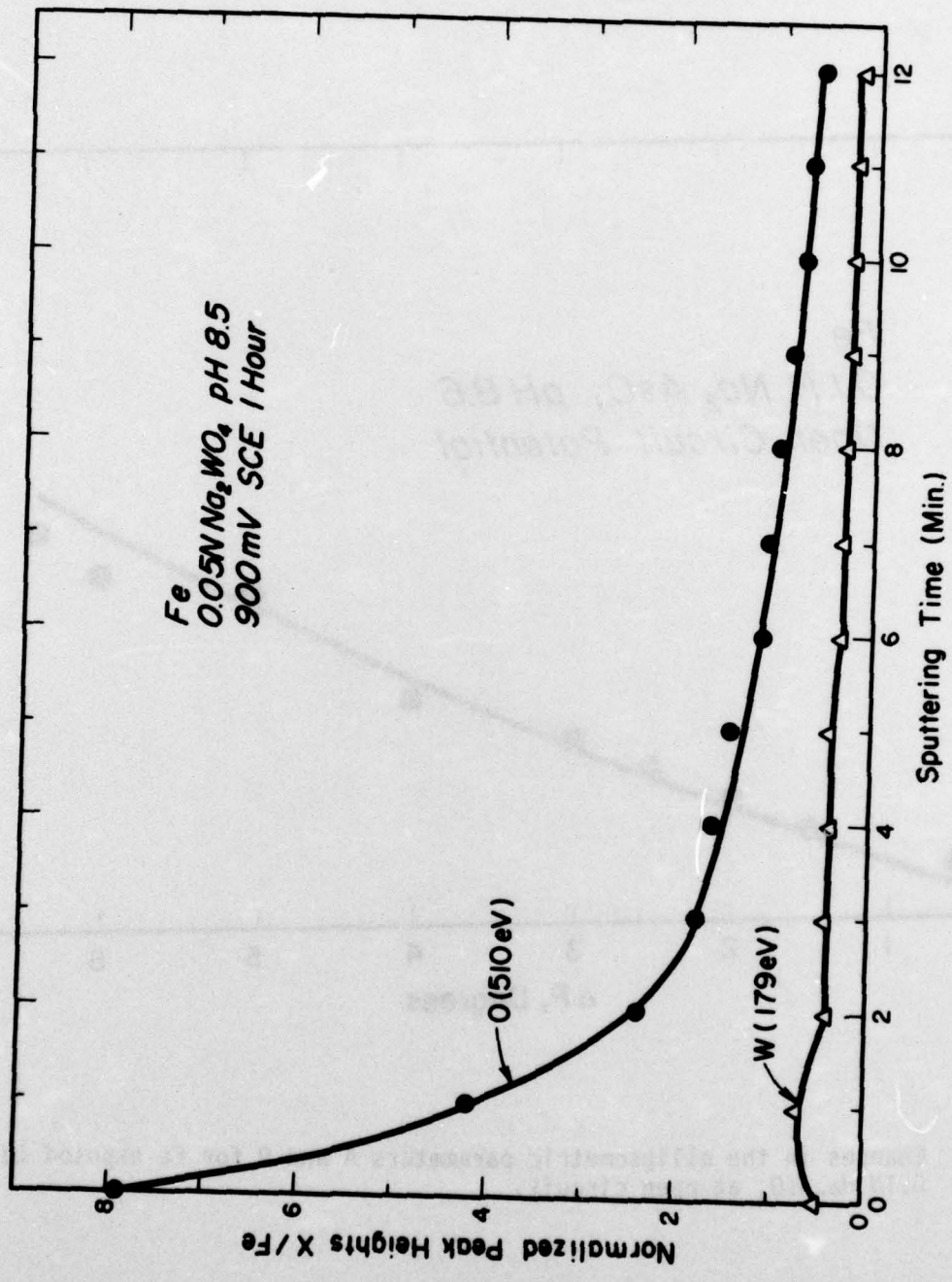


Figure 13 The composition profile of the film formed on Fe exposed to the tungstate solution and at a high anodic potential.

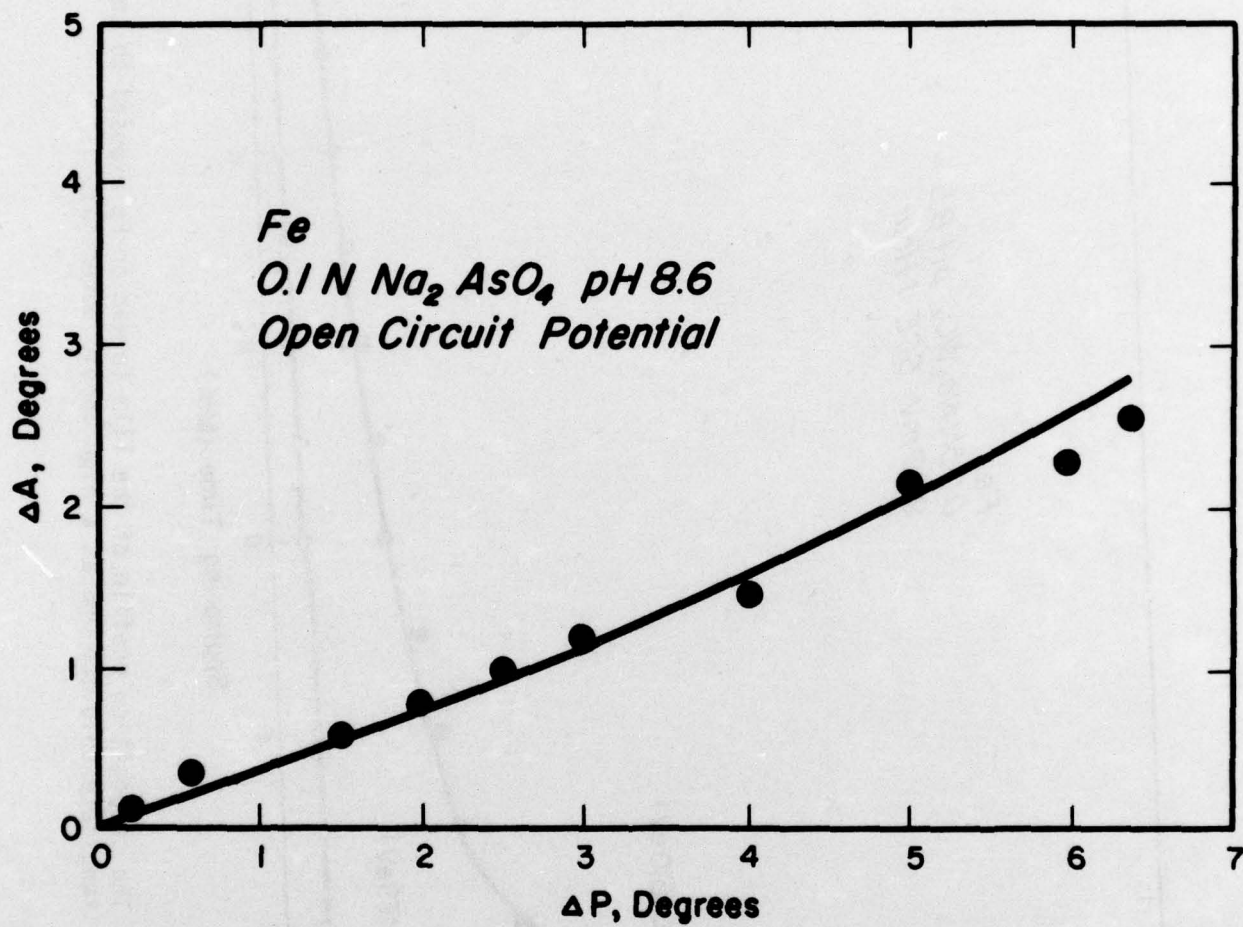


Figure 14 Changes in the ellipsometric parameters A and P for Fe exposed to 0.1N Na₂AsO₄ at open circuit.

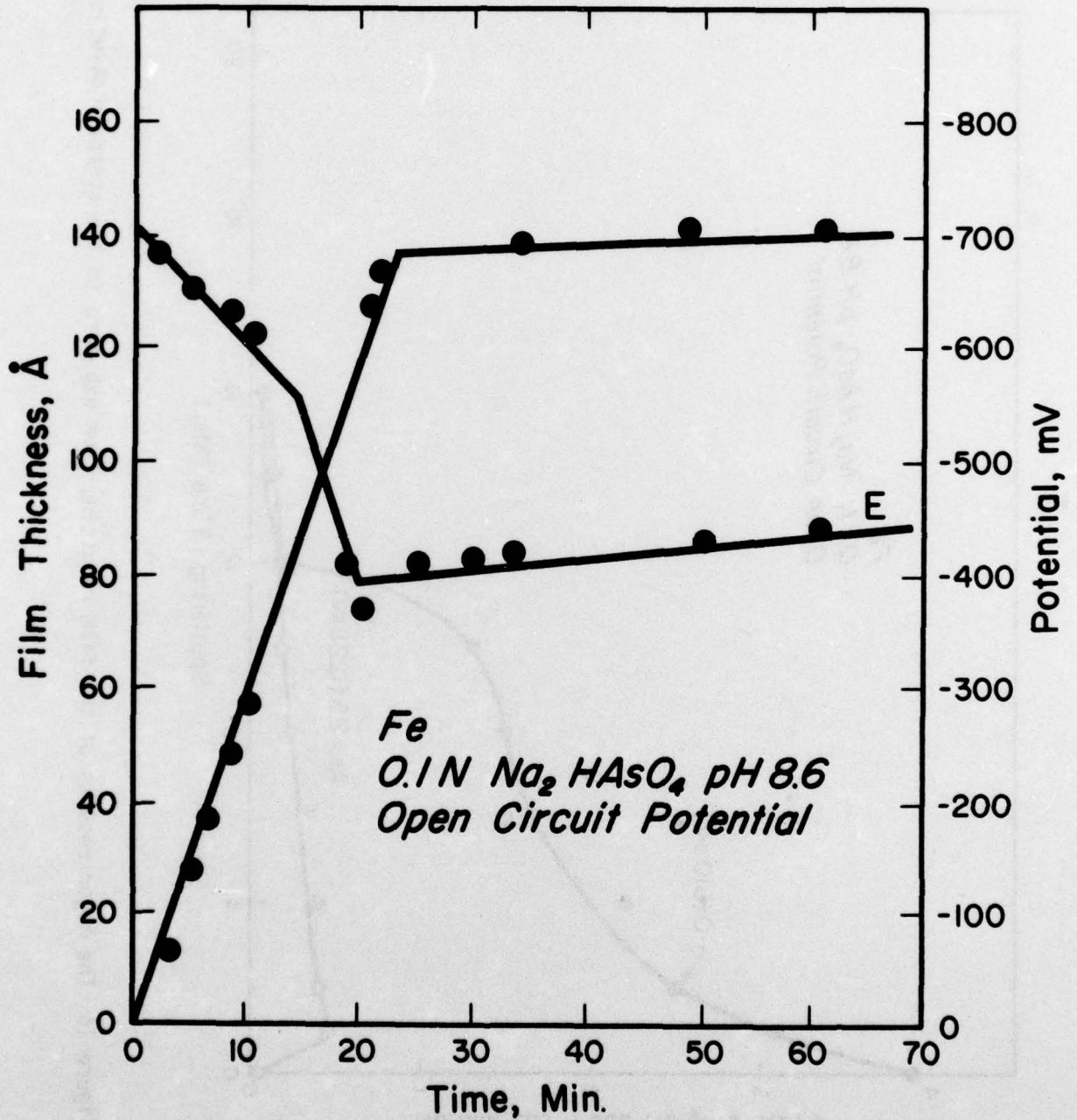


Figure 15 The film thickness and open circuit potential vs. time for Fe in the arsenate solution.

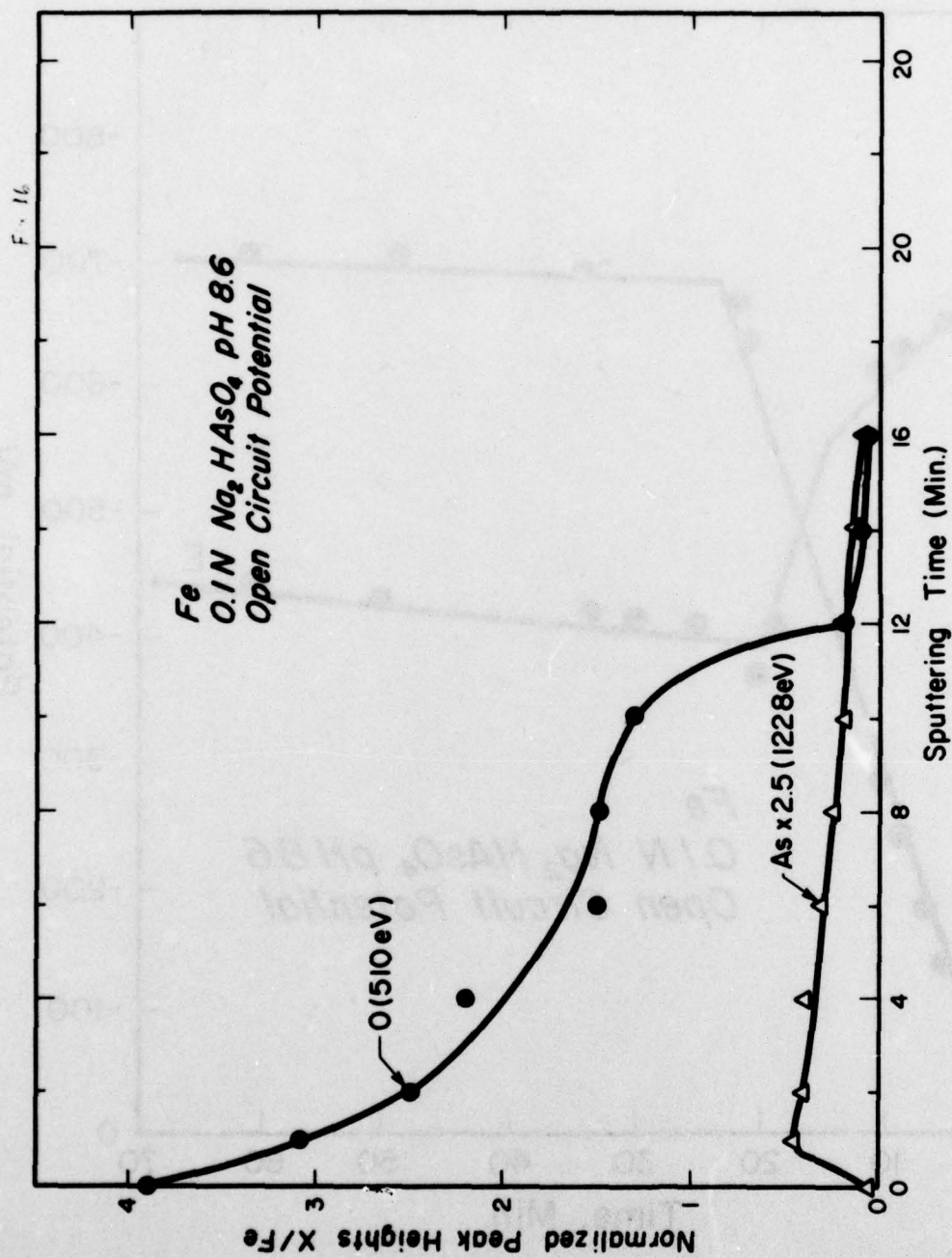


Figure 16 The Auger results of the film resulting from exposure to the arsenate solution.

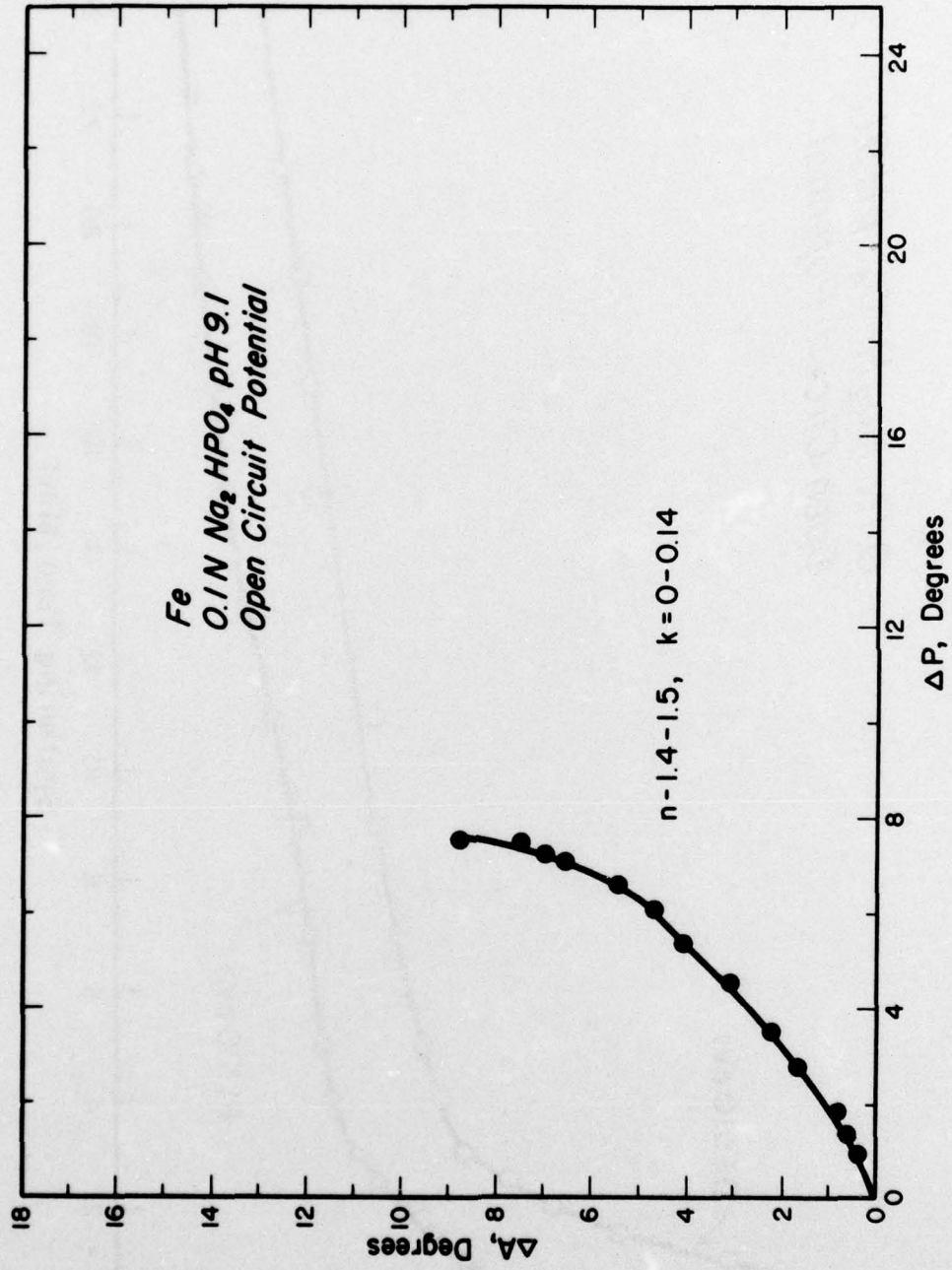


Figure 17 The ellipsometric results for Fe exposed to 0.1N Na₂HPO₄ at open circuit potentials.

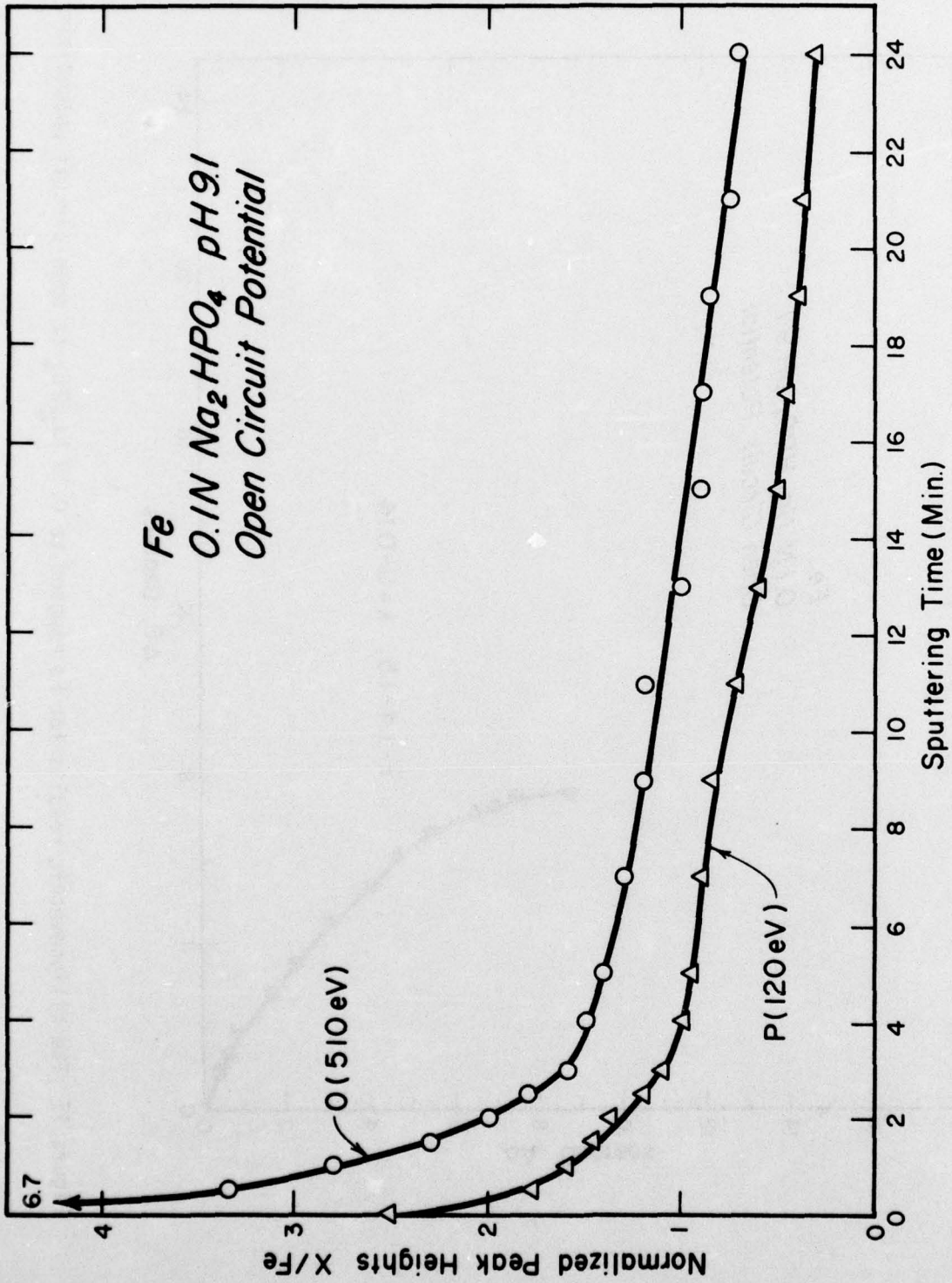


Figure 18 The composition of the film formed by immersion in 0.1N Na₂HPO₄ at open circuit potentials.

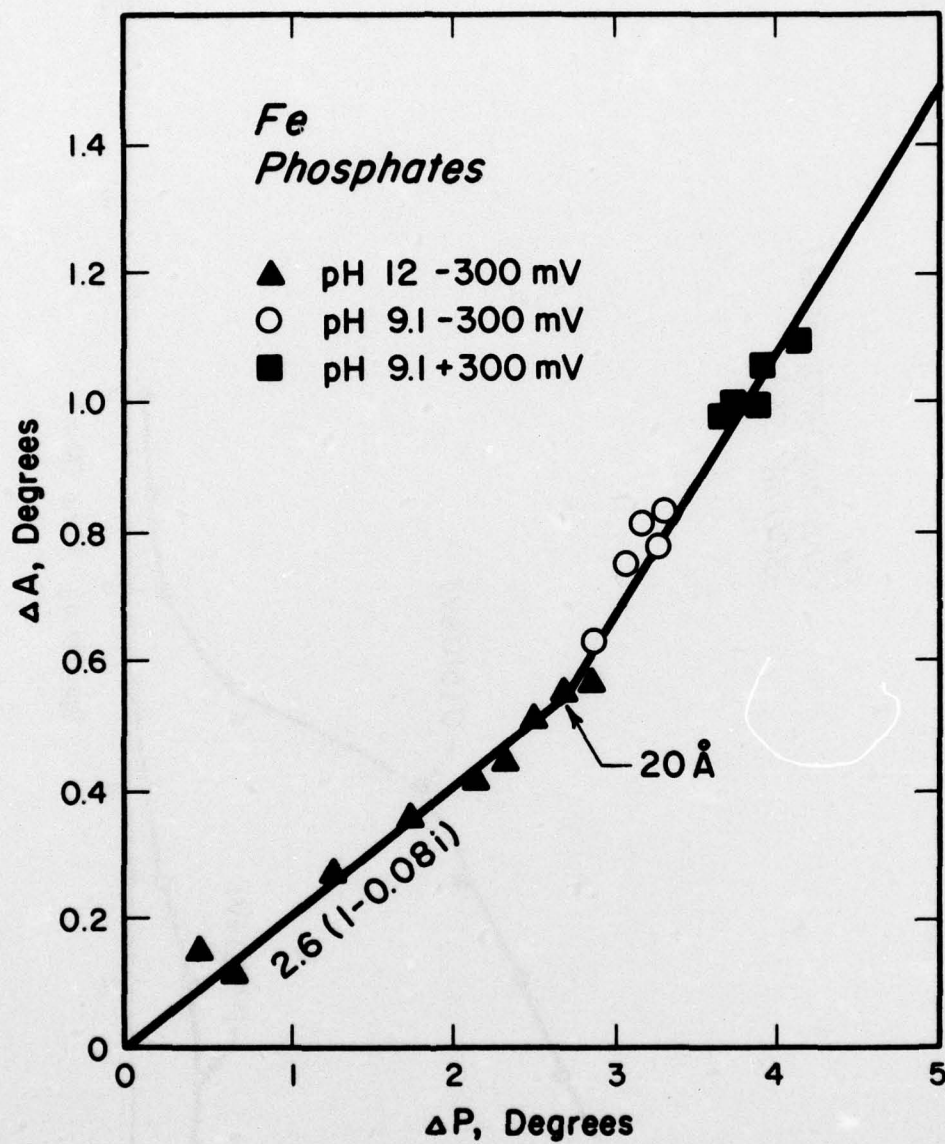


Figure 19 The ellipsometric results for Fe exposed to phosphates and at applied anodic potentials.

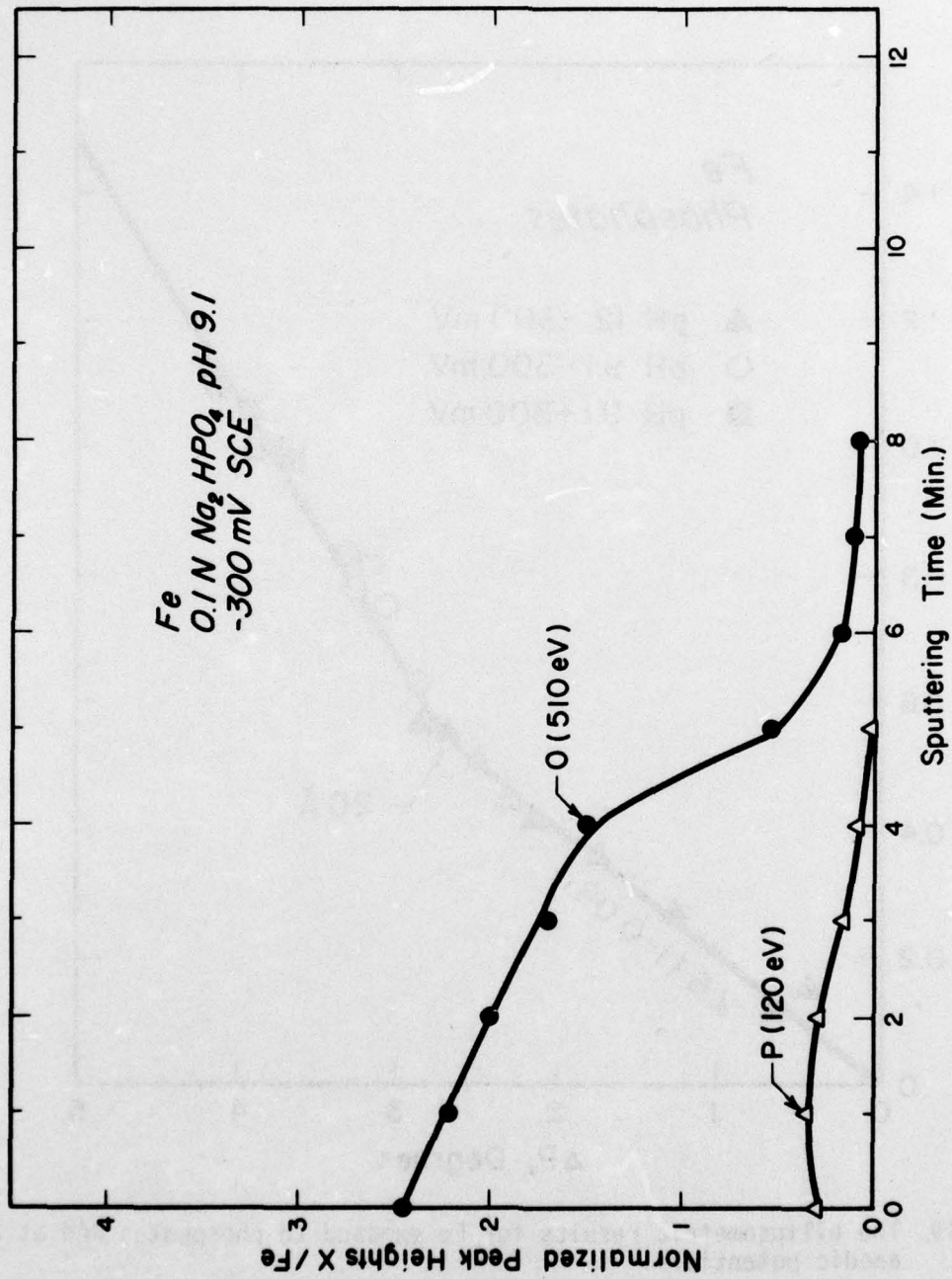


Figure 20 The composition profile of the film formed on Fe at -300 mV (SCE) in Na_2HPO_4 .

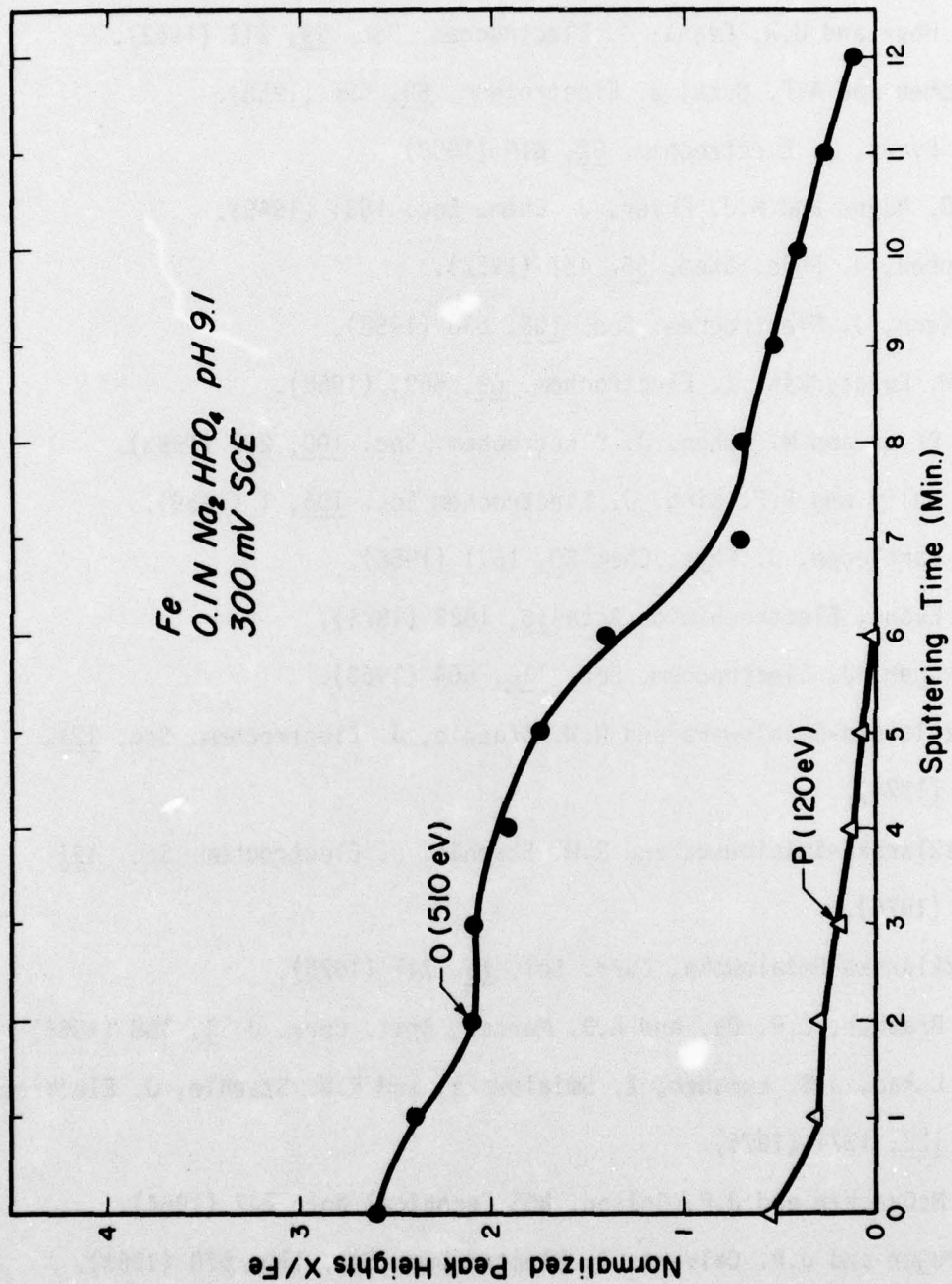


Figure 21 The composition profile of the film formed on Fe at 300 mV (SCE) in Na₂HPO₄.

REFERENCES

1. T.P. Hoar and U.R. Evans, J. Chem. Soc. 2476 (1932).
2. T.P. Hoar and U.R. Evans, J. Electrochem. Soc. 99, 212 (1952).
3. M. Cohen and A.F. Beck, Z. Electrochem. 62, 696 (1958).
4. U.R. Evans, Z. Electrochem. 62, 619 (1958).
5. J.E.O. Mayne and M.J. Pryor, J. Chem. Soc. 1831 (1949).
6. M. Cohen, J. Phys. Chem. 56, 451 (1952).
7. M. Stern, J. Electrochem. Soc. 105, 638 (1958).
8. Ya. M. Kolotyrkin, Z. Electrochem. 62, 669, (1958).
9. M.J. Pryor and M. Cohen, J. Electrochem. Soc. 100, 202 (1953).
10. H.H. Uhlig and P.F. King, J. Electrochem Soc. 106, 1 (1959).
11. G.H. Cartledge, J. Phys. Chem 60, 1571 (1956).
12. U.R. Evans, Electrochimica Acta 16, 1825 (1971).
13. J. Kruger, J. Electrochem. Soc. 110, 664 (1963).
14. Z. Szklarska-Smialowska and R.W. Staehle, J. Electrochem. Soc. 121, 1393 (1974).
15. Z. Szklarska-Smialowska and R.W. Staehle, J. Electrochem. Soc. 121, 1146 (1974).
16. Z. Szklarska-Smialowska, Corr. Sci. 15, 741 (1975).
17. D.M. Brasher, C.P. De, and A.D. Mercer, Brit. Corr. J. 1, 188 (1966).
18. C.N. Lukac, J.B. Lumsden, Z. Smialowska, and R.W. Staehle, J. Electrochem. Soc. 122, 1571 (1975).
19. F.L. McCrackin and J.P. Colson, NBS Technical Note 242 (1964).
20. J. Kruger and J.P. Calvert, J. Electrochem. Soc. 110, 670 (1963).
21. J.L. Ord and D.J. DeSmet, *ibid.*, 113, 1258 (1966).

22. N. Sato and K. Kudo, *Electrochimica Acta* 16, 447 (1971).
23. H.T. Tolken and J. Kruger, *J. Opt. Soc. Am.* 55, 842 (1955).
24. M. Seo, N. Sato, J.B. Lumsden, and R.W. Staehle, *Corrosion Science*,
in press.
25. C.N. Lukac, Z. Smialowska, J.B. Lumsden and R.W. Staehle, *Corrosion Science*,
in press.
26. P.W. Palmer, G.E. Riach, R.E. Weber, N.C. MacDonald, "Handbook of
Auger Electron Spectroscopy", Physical Electronics Industries, Inc. (1972).
27. J.B. Lumsden and R.W. Staehle, ASTM STP 596 (1976).